RI URBANS

HORIZON 2020

European Commission

Guidance documents on measurements and modelling of novel air quality pollutants:

Source apportionment of eBC, UFP, OP and VOCs

with the support of:

AXA Research Fund

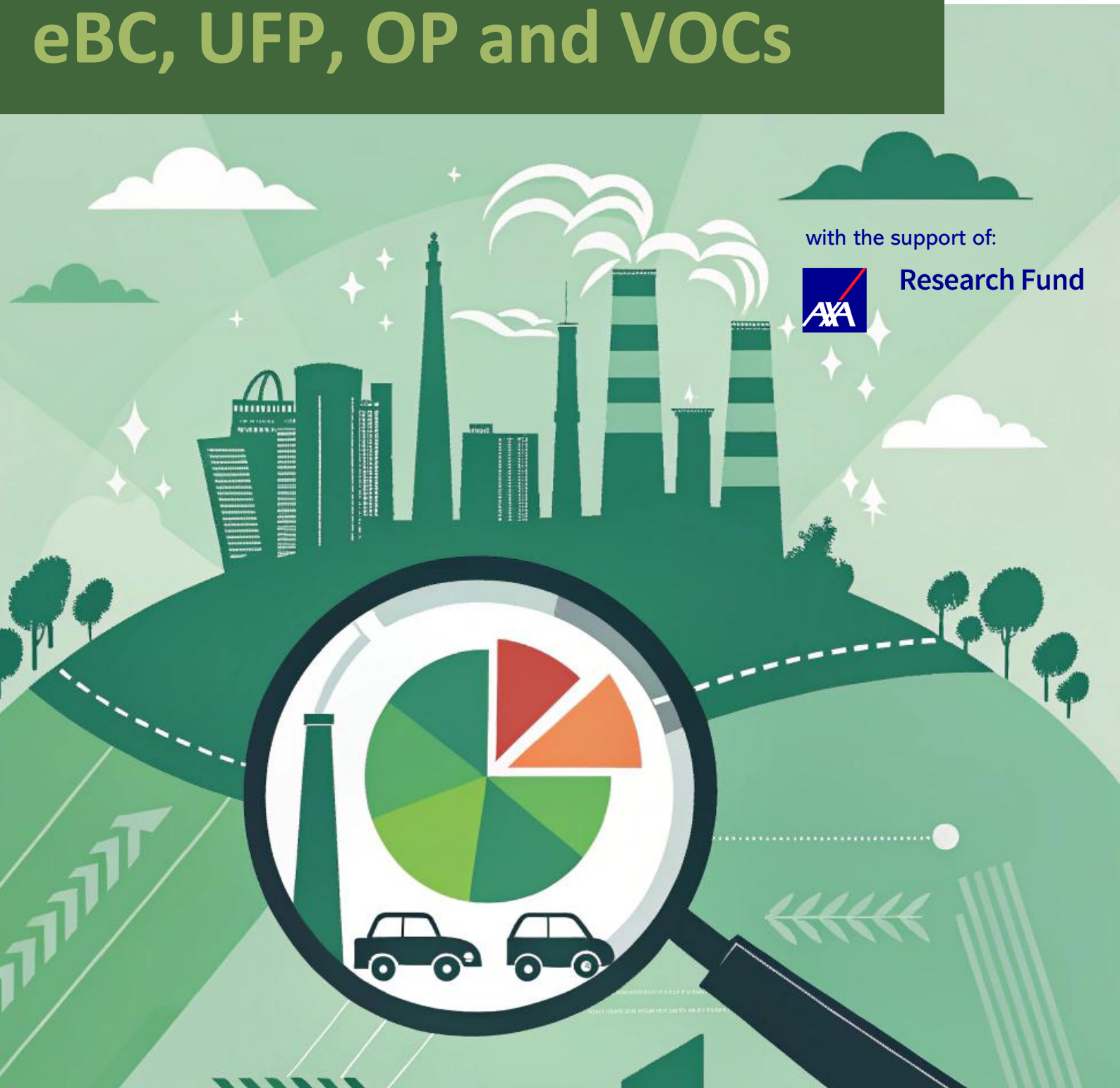

BC source apportionment: Marjan Savadkoohi (CSIC), Marco Pandolfi (CSIC), Olivier Favez (INERIS), Mohamed Gherras (INERIS), Andres Alastuey (CSIC), Tuukka Petäjä (UHEL), Xavier Querol (CSIC)

UFP source apportionment: Meritxell Garcia-Marlès (CSIC), Phil Hopke (University of Clarkson), Roy Harrison (UoB), Andres Alastuey (CSIC), Tuukka Petäjä (UHEL), Xavier Querol (CSIC)

Oxidative potential of PM source apportionment: Gaëlle Uzu (IGE), Kaspar Daellenbach (PSI), Vy Dinh Ngoc Thuy (IGE), Andre Prevot (PSI), Jean-Luc Jaffrezo (IGE)

VOC source apportionment: Thérèse Salameh (IMT Nord Europe - author), Marvin Dufresne (IMT Nord Europe), Marten In't Veld (CSIC, RIVM), Stéphane Sauvage (IMT Nord Europe), Michelle Jessy Müller (EMPA), Stefan Reimann (EMPA)

Reviewers: Xavier Querol (CSIC), Katriina Kyllönen (FMI), Imre Salma (ELTE), Olivier Favez (INERIS), Hilkka Timonen (FMI), Heidi Hellén (FMI), Elli Suhonen (FMI)

Cover image created with AI using RECRAFT

Research Infrastructures Services Reinforcing Air Quality Monitoring Capacities in European Urban & Industrial AreaS (RI-URBANS)

RI-URBANS (http://www.RIURBANS.eu) is supported by the European Commission under the Horizon 2020 – Research and Innovation Framework Programme, H2020-GD-2020, Grant Agreement number: 10103624

Table of Contents

Abbreviations

AAE	Absorption Ångström exponent
ACSM	Aerosol chemical speciation monitor
ACTRIS	Aerosols, Clouds and Trace gases Research InfraStructure
ACTRIS–CiGas	ACTRIS Centre for Reactive Trace Gases In Situ Measurements
AE	Aethalometer
BB	Biomass burning
BC	Black carbon
BrC	Brown carbon
BTEX	Benzene, toluene, ethylbenzene, and xylenes
CMB	Chemical mass balance
CPF	Conditional probability function
CTM	Chemical transport model
DPF	Diesel particulate filters
eBC	Equivalent black carbon
EC	Elemental carbon
FAIRMODE	The Forum for Air quality Modelling, a network of European modelers chaired by JRC
FOX	Ferric-xylenol orange
GC-FID	Gas chromatography flame ionisation detector
H*	Harmonization factors
JRC	Joint Research Centre (in EU)
LF	Liquid fuel combustion
m/z	Mass per charge
LoD	Limit of detection
MLP	Multilayer perceptron
MLR	Multiple linear regression analyses
MS	Mass spectrometry
NMHC	Non-methane hydrocarbons
NPF	New particle formation
OA	Organic aerosols
OC	Organic carbon
OLS	Ordinary least squares
OP	Oxidative potential
OVOC	Oxygenated volatile organic compounds
PAH	Polycyclic aromatic hydrocarbons
PCA	Principal component analysis
PDF	Probability density function
PM	Particulate matter
PM_1	Mass concentration of particles <1 µm
$PM_{2.5}$	Mass concentration of particles <2.5 µm
PM_{10}	Mass concentration of particles <10 µm
PM_x	PM_{10}, $PM_{2.5}$ and PM_1, indistinctively
PMF	Positive Matrix Factorization, a receptor model for source apportionment
PNC	Particle number concentration
PNSD	Particle number size distribution
PTR	Proton transfer reaction

QMS	Quadrupole mass spectrometer
RF	Random forest
RB	Regional background
RI-URBANS	Research Infrastructures Services Reinforcing Air Quality Monitoring Capacities in European Urban & Industrial AreaS EU-project
ROS	Reactive oxygen species
S/N	Signal-to-noise ratio
SA	Source apportionment
SF	Solid liquid combustion
SUB	Sub-urban background
SVOC	Semi-volatile organic compound
ToF-MS	Time of flight mass spectrometry
TR	Traffic
UB	Urban background
UFP	Ultrafine particles
US-EPA	United States Environmental Protection Agency
UV-VIS	Ultraviolet–visible (regions of the electromagnetic spectrum)
VOC	Volatile organic compound

Chemical species

AA	Ascorbic acid
DCFH	Dichlorodihydrofluorescein
DTT	Dithiothreitol
LG	Levoglucosan
MACR	Methacrolein
MEK	Methyl ethyl ketone
MSA	Methanesulfonic acid
MVK	Methyl vinyl ketone

1. ABOUT THIS DOCUMENT

Source apportionment (SA) is a common modelling exercise aimed at identifying main sources of pollutants, and quantifying source contributions. This can be done for atmospheric pollutants, such as particulate matter (PM), but also for its components, by using direct or receptor modelling. Among the diverse SA receptor modelling techniques, Positive Matrix Factorization (PMF) is the most widely used model that uses the time-series concentrations (and their uncertainties) of multiple PM components to identify the main factors/sources responsible for their variations. However, other approaches can allow receptor modelling for SA.

In another guidance document (ST10), RI-URBANS reports on the SA of PM and PM components using PMF, and input data from both offline (sampling and post-analyses at laboratories) and online measurements. This document offers an overview of the best available procedures for performing SA analysis of equivalent black carbon (eBC), particle number concentration (PNC) from particle number size distribution (PNSD), oxidative potential (OP) of PM and volatile organic compounds (VOCs).

This is a RI-URBANS/ACTRIS guidance for this specific service tool that is part of the RI-URBANS deliverable D46 (D6.1, containing guidance for all service tools provided in the project) with the support for publication from AXA Research Fund to build up the final dissemination D55 (D7.6). Any dissemination of results must indicate that it reflects only the author's view and that the European Commission is not responsible for any use that may be made of the information it contains.

2. eBC SOURCE APPORTIONMENT

2.1. Review on eBC source apportionment methods

eBC is used in the present document (instead of BC, for instance) to refer to the concentration of black carbon containing particles estimated from filter absorption photometer, following the recommendations of Savadkoohi et al. (2024) and as also detailed in the Service Tool ST2 of RI-URBANS (https://riurbans.eu/project/#service-tools).

An increasing number of SA studies has reported the proportion of eBC originating from liquid fuel combustion (e.g., vehicular exhaust emissions; eBC_{LF}) and solid fuel combustion (primarily from residential and commercial wood and coal burning; eBC_{SF}) across different urban, traffic, and regional background environments. Such eBC source apportionment (eBC-SA) efforts are of outmost importance due to the potential health and climate impacts of soot (Blanco-Donado et al., 2022; Grange et al., 2020; Helin et al., 2018; Kumar et al., 2020; Liakakou et al., 2020; Milinković et al., 2021; Mousavi et al., 2018, 2019; Sandradewi et al., 2008; Favez et al., 2009; Segersson et al., 2017; Titos et al., 2017).

The most commonly-used and operational eBC-SA method is the so-called Aethalometer model (AE model), consisting of a bilinear approach that uses source-specific absorption Ångström exponents (AAEs) derived from experimental measurements or established literature values (Sandradewi et al., 2008; Zotter et al., 2017). The AAE is an optical parameter that describes the spectral dependence of light absorption by aerosols. An AAE of around 1 indicates that the absorption is dominated by pure black carbon containing aerosols, while a progressive increase in AAE is associated with an increasing contribution of other types of absorbing components such as brown carbon (BrC) or mineral dust (Zhang et al., 2020a, 2020b). AAEs spectra are derived for specific types of eBC sources, such as vehicular emissions, biomass burning (BB), coal combustion, industrial or shipping emissions (Helin et al., 2021; Basnet et al., 2024). However, there are certain limitations to consider when using the AE model. The output of this model is highly sensitive to the input of AAEs. The method relies on accurate calibration factors and representative AAEs for different sources, which may introduce uncertainties. The AE model assumes that the absorption properties of eBC remain constant, irrespective of aging or mixing with other aerosol components. However, variations in the mixing state and aging processes of soot can impact the accuracy of SA results due to changes of characteristics of optical properties of a specific source over time (Harrison et al., 2013; Helin et al., 2021; Luo et al., 2023; Virkkula, 2021).

Several experimental studies have highlighted challenges regarding the reliability of the estimations derived from the AE model. This model was originally developed in a region accounting for only two predominant sources of eBC: biomass burning and fossil fuel combustion primarily linked to traffic (Sandradewi et al., 2008). The most widely used AAE values are the ones recommended by Sandradewi et al. (2008) and Zotter et al. (2017). These values ($AAE_{fossil\ fuel}$ = 1.0 or 0.9 and AAE_{BB}= 2.00 or 1.68) have been obtained in Switzerland with a significant contribution from BB emissions.

However, a robust AAE value may vary over location and time depending on the type of fuel burnt and the combustion conditions and efficiency including emissions from shipping, coal, traffic and residential wood burning (Helin et al., 2021). In addition, AAE value is sensitive to both particle geometry, morphology and size distribution. Overall, it can range from 0.8 to 1.3 for "pure eBC", and reaches values up to more than 2.0 when eBC is co-emitted with BrC (Virkkula, 2021; Ferrero et al., 2021; Li et al., 2016; Liu et al., 2018; Luo et al., 2023). Therefore, the eBC-SA results obtained through the use of AE models can exhibit bias, attributable to AAE values that are relatively higher or lower in magnitude (Harrison et al., 2013; Helin et al., 2021; Zotter et al., 2017). There are studies that have recommended the use of the AAE probability density function (AAE PDF) as an alternative method to estimate site-specific AAE values (Tobler et al., 2021; Glojek et al., 2024; Savadkoohi et al., 2023). With this approach the AAE is calculated from multi-wavelength absorption measurements (e.g. from aethalometers) as linear fit between the measured absorption coefficients and the corresponding wavelengths in a log-log space. Then, a visual inspection of the AAE PDF is performed to estimate site-specific AAE values considering that the tails of the AAE PDF end at the values that represent the local AAEs that can be used in the AE model. This methodology is recommended here for eBC-SA, as described in the following sections and after a brief description of alternative approaches sometimes used for research activities.

As mentioned in introduction, PMF is a widely used technique for aerosol source apportionment in air pollution studies (Grange et al., 2020; Liu et al., 2022; Masiol et al., 2019; Massabò and Prati, 2021; Rivas et al., 2019; Squizzato et al., 2018; Tobler et al., 2021; Wang et al., 2021). PMF is a receptor model that aims at identifying and quantifying the contributions of different sources to ambient concentrations. It may use eBC along with additional data such as PM chemical composition, particle size distribution, and meteorological data. The advantages of PMF for eBC-SA include its ability to identify distinct emission sources, even in complex atmospheric environments with multiple source contributions. It can provide quantitative estimates of source contributions and help in understanding the spatial and temporal variations of a wide set of eBC sources. However, like any other modelling technique, PMF has certain limitations. The accuracy of the results depends on the quality and representativeness of the input data matrices, including the measurement and related uncertainty datasets. Model assumptions and parameter selection can also highly influence the results. Moreover, interpretation of the factors requires expert knowledge and careful consideration of potential cofounding factors (Hopke, 2016; Hopke et al., 2023).

Other previous studies have employed different methodologies to compare the outcomes of the AE model with SA results using offline auxiliary measurements such as levoglucosan (LG), elemental carbon (EC), radiocarbon (^{14}C), or a combination of different SA methods such as coupled radiocarbon-levoglucosan marker method to effectively attribute carbonaceous aerosol (Salma et al., 2017). For instance, Bibi et al. (2021) and Zheng et al. (2021) have recently employed a combination of PMF and AE modelling techniques. In addition, advanced SA methods are recommended using big data to enhance the analysis and interpretation of eBC-SA results (Hopke et al., 2023). Based on this, several recommendations have been put forth in the literature. Firstly, it is recommended to adopt a multi-tracer approach or macro-tracer method that combines eBC measurements with other complementary measurements, such as EC, OC, and other chemical species (Briggs and Long, 2016; Fourtziou et al., 2017). Nevertheless, these types of measurements are not extensively accessible at all monitoring sites. Secondly, the use of high-resolution time series measurements is needed to capture the temporal variability of eBC sources to identify diurnal, weekly, and seasonal patterns, and quantify different source contributions especially for human exposure assessments (Gregorič et al., 2020; Hamilton and Harley, 2021). To ensure the comparability of results across different studies, it is essential to report detailed information on filter absorption measurement techniques, instrument calibration, data quality control, and uncertainty estimation.

2.2. Overview of eBC source apportionment studies on selected EU urban sites

To evaluate the relative contributions of eBC_{SF} and eBC_{LF} in urban Europe, the AE model was applied to data from 23 monitoring sites between 2017–2019 extracted from the RI-URBANS database. This study followed the conventional approach of using fixed AAE values for the SA of AE33 observations due to the lack of ancillary measurements such as ^{14}C that could be used to determine site-dependent AAEs. Thus, AAE values of 1.00 and 0.90 were used for eBC_{LF}, while AAE values of 2.00 and 1.68 were used for eBC_{SF} for the 470–950 nm wavelengths, respectively (Sandradewi et al., 2008; Zotter et al., 2017). The obtained results of relative contributions of eBC_{SF} and eBC_{LF} using two sets of fixed AAE values were compared to evaluate the variations across different regions due to the limitation of constant AAE values (Savadkoohi et al., 2023). Figure 1 shows the results of the eBC-SA in Europe. The cities included were: Athens (ATH), Barcelona (BCN), Berlin (BER), Birmingham (BIR), Bucharest (BUC), Granada (GRA), Helsinki (HEL), Hyytiälä (SMR), Lille (LIL), London

(LND), Madrid (MAD), Marseille (MAR), Milano (MLN), Paris (PAR), Stockholm (STH), and Zurich (ZUR). The Figure shows the regional variations in the relative contributions of eBC_{LF} and eBC_{SF} with an increasing trend in the eBC_{LF} from Northern to Central, Western, and South-Western Europe. In general, the relative contribution of solid fuel sources to eBC increased by 25–45% when using the values from Zotter et al. (2017). It should be noted that the AAE values proposed by Zotter et al. (2017) were determined at Swiss sites, strongly influenced by BB emissions. However, based on the available data, it was not definitively concluded which AAE pair (1.00 and 2.00 vs. 0.90 and 1.68) was more appropriate for the sites considered in the study. Thus, it cannot be assumed that the AAE values remain constant across all sites.

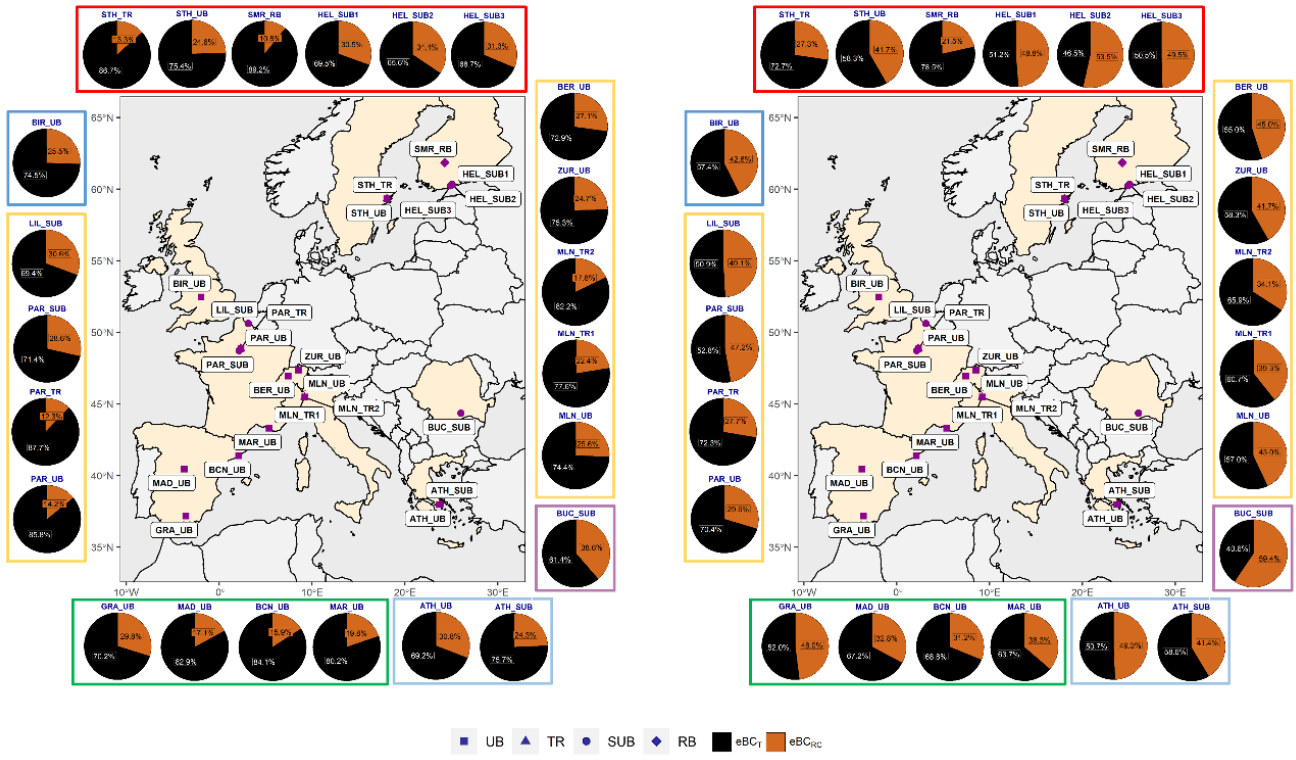

Figure 1. *The results of the SA analysis of eBC mass concentrations for 23 European sites used over 2017–2019. The black color (eBC_T) stands for traffic related eBC (eBC_{LF}), while the brown color (eBC_{RC}) illustrates solid fuel combustion (mainly from residential and commercial wood and coal burning) related eBC (eBC_{SF}). The aethalometer model was applied using (AAE_{LF} = 1.00 and 0.90) for traffic emission sources and (AAE_{SF} = 2.00 and 1.68) for solid and liquid sources. Modified from Savadkoohi et al. (2023).*

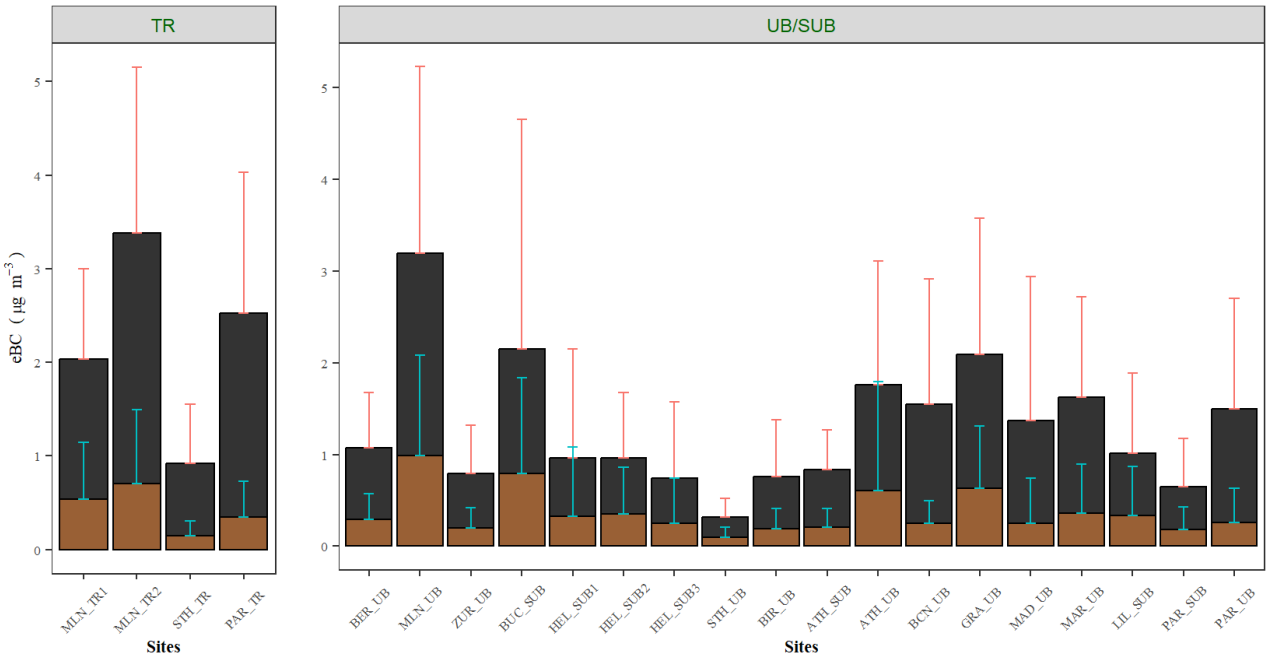

Figure 2. *SA analysis comparing traffic (TR) and urban/suburban (UB/SUB) sites. Variance in the two sources across different sites presented using stacked histograms with error bars. The black color stands for traffic related eBC (eBC_{LF}), while the brown color illustrates solid fuel combustion (mainly from residential and commercial wood and coal burning) related eBC (eBC_{SF}). Modified from Savadkoohi et al. (2023).*

2.3. Recommendations for eBC source apportionment

The methodology for eBC determination using aethalometers, including all steps to harmonize absorption measurements, is comprehensively detailed in the guidelines document for eBC (see the RI-URBANS guidance document for measurements of eBC document, ST2, in https://riurbans.eu/project/#service-tools). This includes all relevant theory and calculations. Here, we focus only on the recommendations for applying the AE model for eBC-SA purposes.

2.3.1. Selection of AAE_{LF} and AAE_{SF} for eBC source apportionment

For the application of the AE model, the source-specific absorption AAEs factor for liquid (AAE_{LF}) and solid (AAE_{SF}) fuel combustion have to be selected. The AE model is based on the fact that solid fuel sources emit eBC together with some specific organic aerosols (OA) that can absorb in the UV-VIS spectral range (the so-called brown carbon, BrC), thus causing an increase of AAE. Conversely, it is commonly assumed that BrC is not emitted, or it is emitted in very low amounts, from liquid fuel combustion sources such as traffic and that the AAE is close to one. Usually, two pairs of values are used: 1.0 and 2.0 for AAE_{LF} and AAE_{SF}, respectively, or 0.90 and 1.68, respectively (Sandradewi et al., 2008; Zotter et al., 2017). The latter values from Zotter et al. (2017) were calibrated using ^{14}C measurements and may be considered as the values to be used where traffic and BB are the only

sources of eBC. However, other solid sources than biomass burning (e.g., coal combustion), or liquid fuel sources as shipping, can emit BrC but the AAE_{SF} associated to these sources has been poorly characterized. Laboratory studies have shown that especially for heavy fuel oil combustion the AAE can be >2 (Helin et al., 2021).

The AAE can be calculated as the linear fit in a log-log space between the seven harmonized absorptions from AE instruments and the corresponding wavelengths. The model performance was investigated using site-dependent AAE_{LF} and AAE_{SF} determined from measurements in ambient air. To do this, we calculated the 1st and 99th percentiles of the experimental AAE values and associated them to the AAE_{LF} and AAE_{SF}, respectively, needed for BC-SA. Only AAE values obtained from fits with R^2>0.99 should be used to calculate the 1st percentile, whereas unfiltered AAE values should be used to calculate the 99th percentile. Moreover, in order to minimize the contribution to absorption from BrC sources, the 1st percentile should be calculated using summer absorption data. Conversely, and in order to maximize the contribution from BrC sources, winter data should be used to calculate the 99th percentile. This minimization/maximization of BrC sources is based on the fact that BrC emissions from BB maximize in winter. This approach is similar to the approach proposed by Tobler et al. (2021) with the main difference that here we used the 1st and 99th percentiles instead of a simple visual inspection of the AAE PDF. As an example, a sensitivity study was performed using simultaneous absorption measurements at three monitoring sites in Barcelona and at one site in a small town (Manlleu, NE Spain) where the latter was affected by traffic and high BB emissions. In contrast, the BCN measurement sites were much less affected by BB emissions than Manlleu, while road traffic together with industries, power plants, and the port of Barcelona represent the main sources of eBC at these sites. In addition, there is a strong influence from sea breezes, which can transport traffic-related pollution into the city (Veld et al., 2021). Thus, in BCN, shipping emissions can be considered as an important source of BrC. Despite ships burning fossil liquid fuels, the emissions classified as fossil-based eBC actually fell into the category of solid fuel especially if high sulphur content heavy fuel oil was used (e.g. Helin et al., 2021). Considering this, shipping emissions can represent a significant source of light-absorbing OAs, particularly in port areas. As a result, precisely defining liquid and solid sources of eBC to accurately attribute emissions from different sources is important.

Figure 3 shows the frequency distributions of the AAE for different locations: BCN_Port, BCN_TR, BCN_UB, and Manlleu based on eBC concentration. At BCN_Port, the 1st percentile was 1.02, and the 99th percentile was 2.01, confirming the contribution of shipping emissions to both eBC and BrC.

Recently, Helin et al. (2021) reported AAE values up to 2.0 ± 0.1 for shipping emissions using high sulphur content heavy fuel oil. The eBC concentration at BCN-Port showed higher values in the left tail of the PDF, which can be attributed to low AAE values associated with liquid fuel sources, such as traffic emissions. At BCN_TR, the 1st percentile was 1.05, and the 99th percentile was 1.49. The concentration of eBC showed variability with a higher concentration in left tile associated with traffic and liquid fuel sources. Based on our observation, the 99th percentile calculated for example at traffic sites with low impact from solid sources can often be too low (e.g., < 1.4–1.5), thus resulting in an overestimation of solid fuel contribution to eBC from the AE model. Thus, the 99th percentile should be used with cautions and only at sites with significant contribution to absorption from solid sources. At BCN_UB, the 1st percentile was 1.04, and the 99th percentile was 1.6. The eBC is indicated with some high concentration values in the left tile of the PDF. In Manlleu, the 1st percentile was 1.05, and the 99th percentile was 1.72 and eBC showed high concentrations in a wide range of AAE values being slightly more pronounced in the right tile attributed to solid fuels. The AAE_{SF} (i.e. the 99th percentile) obtained in Manlleu was close to the value of 1.68 proposed by Zotter et al. (2017) for a Swiss site strongly affected by BB emissions. Based on the results in Figure 3 from multiple measurement sites in BCN, it can be concluded that the best AAE_{SF} value to apportion eBC in the city was the AAE_{SF} obtained at the port of BCN.

Thus, the values reported above obtained for the 1st percentile aligned with those reported in the literature for fossil, traffic, or liquid sources (i.e. AAE_{LF} around 1). Results indicated that whilst the 1st percentile provided a robust AAE_{LF} for the AE model, the use of the 99th percentile to estimate the AAE_{SF} was limited to those measurement sites with a strong impact from solid fuel sources. Figure 4 presents a series of pie charts that compare the contributions of eBC_{LF} and eBC_{SF} across the considered three types of environments: port, urban, and traffic sites in Barcelona. The comparisons were based on the use of four different AAEs pairs: Sandradewi, Zotter, Frequency Distribution (i.e., 1st and 99th percentiles), and Rolling Percentiles. The Rolling percentiles method involved calculating percentiles within a moving window across a time series of AAE values. This helped understand the temporal distribution and trends of AAE. At BC_Port eBC_{LF} contributions ranged from 44% to 65%, and eBC_{SF} contributions ranged from 35% to 56%. At BCN_UB, the eBC_{LF} contributions ranged from 48% to 67%, and eBC_{SF} contributions ranged from 33% to 52%. At **BCN_TR, t**he eBC_{LF} contributions ranged from 44% to 68%, and eBC_{SF} contributions ranged from 32% to 56%. The results highlighted how the choice of AAE values and methods can significantly affect the apportionment of eBC sources. This variability underscored the importance of method selection and parameter settings in SA studies. For example, Figure 4 shows that the eBC_{SF} contribution to eBC is clearly too high at the traffic site if the 99th percentile or rolling percentile were used to determine the AAE_{sf}. Similarly, the AAE_{SF} proposed by Zotter et al. (2017) for sites strongly affected by BB also led to high and overestimated eBC_{SF} contribution for the traffic site. The eBC_{SF} contribution obtained using the AAEs pair from Sandradewi et al. (2008) led to a more reasonable estimation of eBC_{SF} and eBC_{LF} at BCN_TR. Note also that the AAEs obtained at the BCN_Port using the percentiles were very close to the Sandradewi's AAE values.

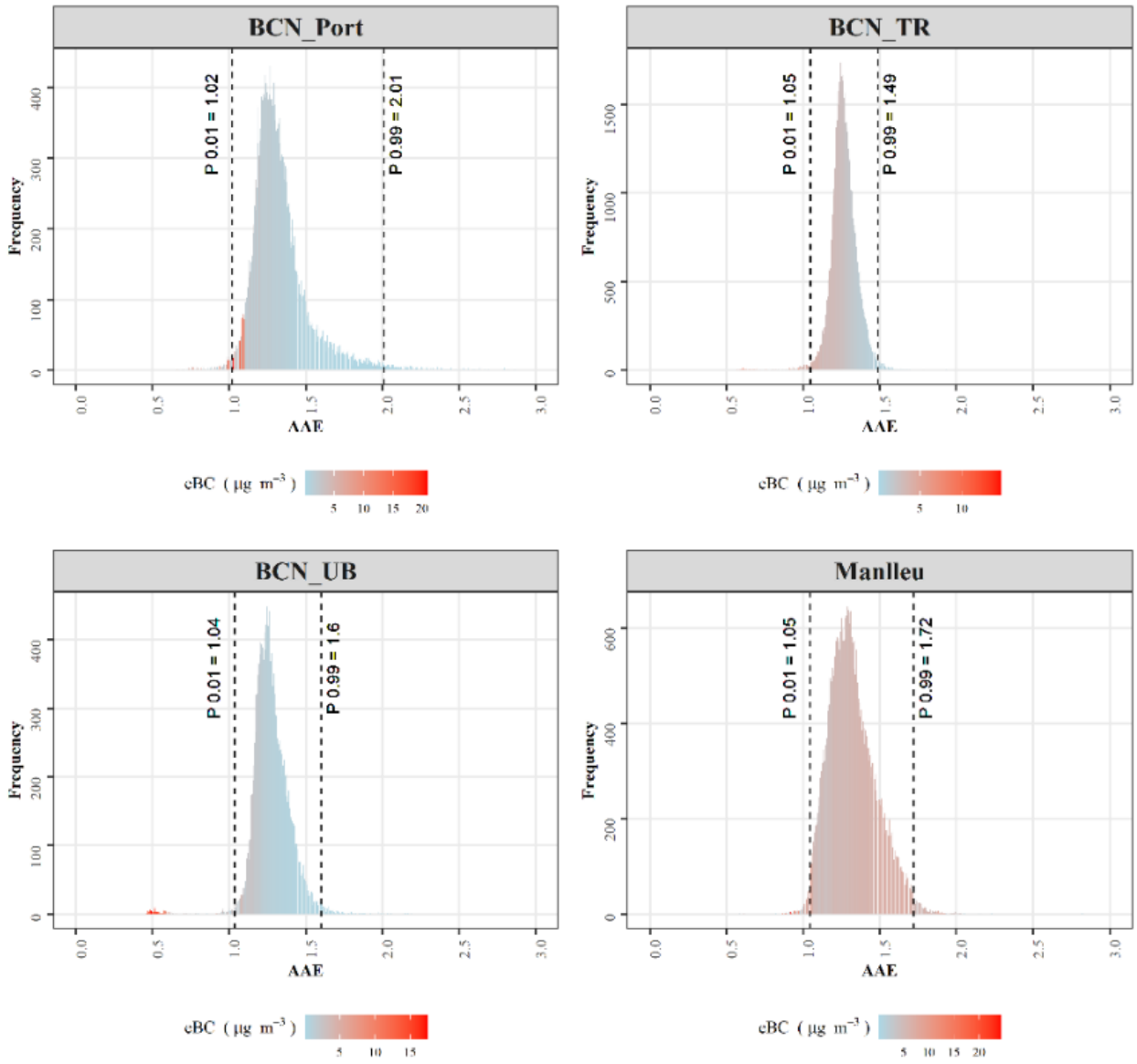

Figure 3. *Simultaneous measurement of eBC at four sites, the AAE_{lf} and AAE_{sf} obtained using 1st and 99th percentile of AAE frequency distribution. Adapted from an ongoing study currently under review by Savadkoohi et al., 2025.*

Figure 4. *Simultaneous aethalometer model results at the port, urban and traffic sites of Barcelona. The black color stands for traffic related eBC (eBC_{LF}), while the brown color illustrates solid fuel combustion related eBC (eBC_{SF}). Zotter AAE values provide too high solid contribution (mathematical consequence of using low AAE_{SF} in the Aethalometer Model). Adapted from an ongoing study currently under review by Savadkoohi et al., 2025.*

Moreover, a sensitivity study using near-real time eBC data from pilot sites was performed in 2023 in order to obtain the site specific AAE values. In this study, the AAE_{SF}, calculated as 99th percentiles, were compared with the AAE_{SF} obtained in an independent way using simultaneous AE and aerosol chemical speciation monitor (ACSM) data. Specifically, ACSM data, including the signal at mass-to-charge ratio (*m/z* 60), may be highly relevant for these analyses. Indeed, *m/z* 60 is often associated

with certain organic compounds produced by solid fuel combustion, such as polycyclic aromatic hydrocarbons (PAHs) and oxygenated organic aerosols. For instance, *m/z* 60 can correlate with BB markers like levoglucosan in many regions. Here, we used *m/z* 60 data from ACSM to determine the AAE_{SF} as explained below. As a first step, we estimated the AAE_{LF} and AAE_{SF} from the 1st percentile of R^2-filtered summer experimental AAE values (from 470 to 950 nm) and from the 99th percentile of unfiltered winter AAE value, respectively. As an example, figure 5 shows the summer and winter AAE PDF and the corresponding AAE_{LF} (1.07) and AAE_{SF} (1.72) for an urban background site in Athens (NOA) strongly affected by BB emissions in winter (e.g., Kaskaoutis et al., 2021).

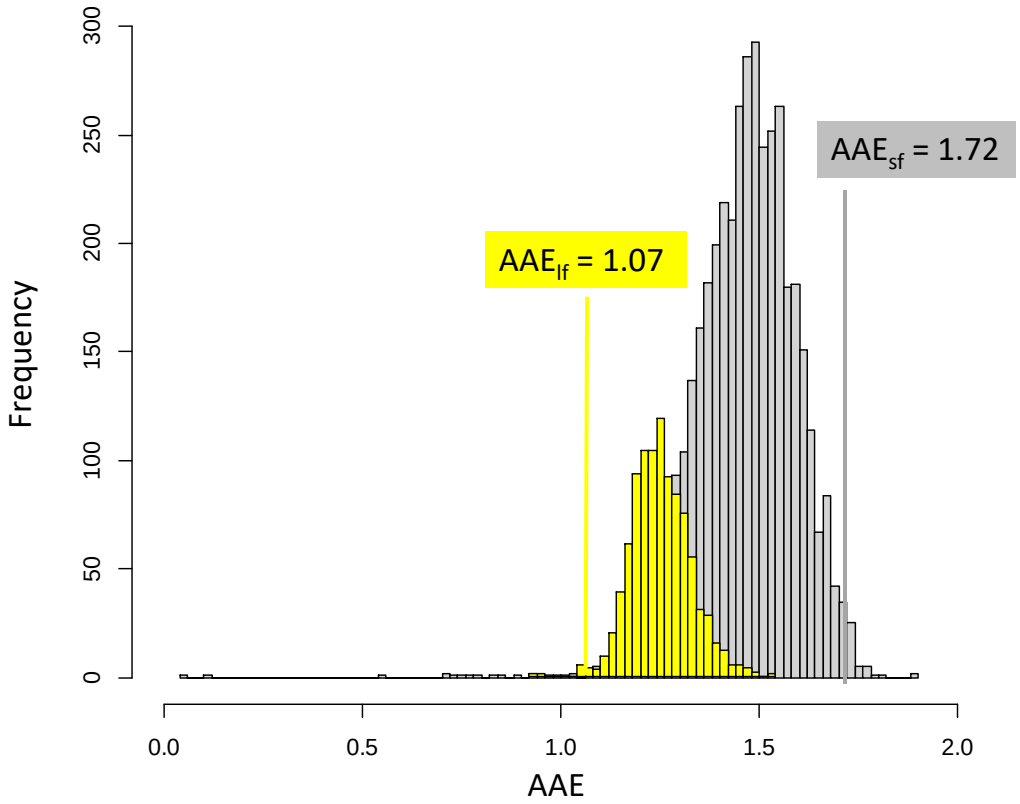

Figure 5. *Experimental AAE PDF obtained at NOA urban site (Athens, Greece). R^2-filtered summer (yellow) and unfiltered winter (grey) AAE PDF are reported together with the corresponding 1st (AAE_{LF}) and 99th (AAE_{SF}) percentiles.* ***Adapted from an ongoing study currently under review by Savadkoohi et al., 2025****.*

In the second step, the Sandradewi model was applied using fixed AAE_{LF} as the 1st percentile and by varying the AAE_{SF} from 1.1 to 2.6. The correlations between the obtained eBC_{SF} and the *m/z* 60 at each site were then studied and the final AAE_{SF} was set as the value for which the highest R^2 in the

eBC_{SF} vs. *m/z* 60 correlation was obtained while intentionally minimizing the correlation for eBC_{LF}. The example for NOA measurement site is reported in Figure 6.

Thus, this approach led to a higher correlation between eBC_{SF} and *m/z* 60, while deliberately seeking a lower correlation for eBC_{LF} and should preferentially be done on wintertime dataset, in order to get sufficient amount of both eBC subfractions in ambient air.

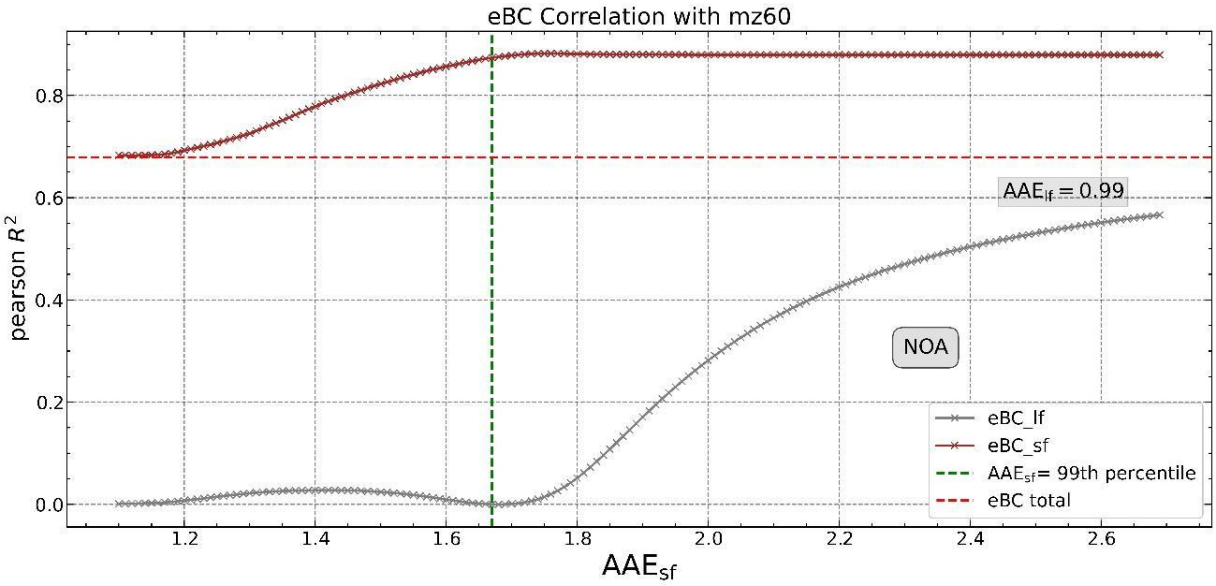

Figure 6. *Correlation of eBC_{LF} and eBC_{SF} fractions with m/z 60 as a function of AAE_{SF} for NOA site.* ***Adapted from an ongoing study currently under review by Savadkoohi et al., 2025.***

As reported in Figure 6 for the NOA measurement site, the optimal AAE_{SF} using the *m/z* 60 was around 1.70–1.72 calculated as the 99th percentile of winter AAE data.

The results of this sensitivity study using data from many measurement sites will be detailed in an upcoming scientific paper, which will combine eBC-SA results obtained in the frame of the RI-URBANS project from both the pan-European overview of historical data and the piloting activities.

2.3.2. Summary and final considerations for eBC source apportionment

Recent findings from the sensitivity study mentioned above revealed a diverse range of values when fixing the lower percentiles and examining the impact of upper percentiles on the coefficient of determination (R^2). Notably, the application of the 1st percentile appeared to be suitable by filtering the R^2. However, uncertainties persist concerning the use of upper 99th percentile, and these

uncertainties could not be addressed completely by exclusively using winter data for AAE estimation.

Comprehensive site characterization, including detailed information about local emission sources, meteorological conditions, traffic patterns, and other relevant factors is necessary to improve the accuracy of eBC-SA results. Use of high-quality and continuous measurements to study the source-specific AAE variation is recommended. Consistent and reliable data are crucial for robust SA. Post-processing of the aethalometer data, considering the ACTRIS procedures and following the recommendations provided by Savadkoohi et al. (2023, 2024) in the framework of the RI-URBANS project is essential. This allowed to harmonize measurements of the wavelength-dependent absorption coefficients ($b_{abs,\lambda}$), recalculated from Attenuation (ATN) measurements provided by the AE33 using harmonization factors (H*) to convert into b_{abs} according to ACTRIS recommendation guidelines. Once corrected in this way, measurements could then be used to quantify the two main eBC subfractions, using the AE model.

In practice, recommending the use of harmonized and fixed AAE values for eBC-SA is not feasible due to the mathematical limitations of the AE model. The AE model primarily provides qualitative rather than quantitative results, making it difficult to achieve robust outcomes. As a result, using fixed and standardized AAE values across different locations or scenarios may not provide reliable and consistent results. The selection of AAE values is reliant on the site operators and can be analysed through the use of collocated eBC measurements with other auxiliary measurements, such as mass-to-charge ratio (*m/z* 60) or ^{14}C. This approach allows for the derivation of robust AAE values adapted to the specific site characteristics. Nevertheless, despite the robustness of this approach, a certain degree of subjectivity may remain in the process.

3. UFP-PNSD SOURCE APPORTIONMENT

3.1. Review on UFP-PNSD source apportionment methods

Ultrafine particles (UFP) can be present in the atmosphere through direct emissions, such as from motor vehicles, or through new particle formation (secondary particles). It is possible to perform source apportionment analysis using receptor models. Typically, receptor models for source apportionment use chemical composition data to provide information on sources of particulate

matter (PM) mass concentrations (Amato and Hopke, 2012; Pancras et al., 2013; Amato et al., 2016; Zíková et al., 2016; Taghvaee et al., 2018). However, sources dominating particle number concentration (PNC) differ from those dominating PM mass concentrations. Thus, several studies have applied receptor modelling for the source apportionment of UFP particle number size distribution (UFP-PNSD), using the variability of the PNSD instead of the chemical composition (Liu et al., 2014; Brines et al., 2014; Beddows et al., 2015; Sowlat et al., 2016; Rivas et al., 2019; Vörösmarty et al., 2024, Hopke et al., 2024). There are only a few studies on source apportionment of UFP compared to larger particles. Hopke et al. (2022) identified 55 peer-review journal papers as reporting source apportionments of PNSD at 102 locations/time periods. Almost all of these studies were performed with Positive Matrix Factorization (PMF), but other methodologies were also used, such as Principal Component Analysis (PCA) and K-Means Clustering.

Pey et al. (2009) performed PCA using STATISTICA v4.2 software on datasets composed of particle number size distributions, meteorological parameters, gaseous pollutants, and chemical speciation of $PM_{2.5}$, following the methodology proposed by Thurston and Spengler (1985). PCA was also used in other studies (Wehner and Wiedensohler, 2003; Chan and Mozurkewich, 2007; Oliveira et al., 2009; Cusack et al., 2013; Khan et al., 2015). Beddows et al. (2009) analyzed the data using K-Means Cluster Analysis, in which the particle size distributions are generalized by cluster types (characteristic of an emission or formation process), facilitating an understanding of the temporal and spatial trends of the size distribution. This method was used in several studies (e.g., Dall'Osto et al., 2011; Wegner et al., 2012; Brines et al., 2014; Brines et al., 2015; Dall'Osto et al., 2019; Chen et al., 2021). Furthermore, Rodríguez and Cuevas (2007) developed a methodology to split PNCs affected by fresh vehicle exhaust emissions into two components: *N1*, accounting for primary particles directly emitted in the particle phase or nucleating immediately after the emissions, and *N2*, accounting for the new particle formation (NPF) and other secondary UFP.

PMF is the most recently used data analysis method to identify and apportion the sources of PNSD. The increased use of PMF came as a result of the freely available implementation provided by the U.S. Environmental Protection Agency (US EPA; Norris et al., 2014). EPA PMF 3.0 (Gu et al., 2011; Wang et al., 2013; Liu et al., 2014; among others) and EPA PMF 5.0 (Squizzato et al., 2019; Dai et al., 2020; Pokorná et al., 2020; among others) are the last versions of PMF Model software, using graphical user interfaces that ease data input, visualization of model diagnostics, and exporting of results. They use the underlying program Multilinear Engine 2 (ME-2, Paatero, 1999) as the factor

analytic problem solver. However, this software does not handle datasets of more than approximately 500,000 data points, and Hopke et al. (2023) has developed a protocol to use the ME-2 for larger datasets without EPA software.

3.2. Source apportionment of UFP-PNSD using Positive Matrix Factorization

Source apportionment of UFP-PNSD for large datasets may be performed by PMF using the tool developed by Hopke et al. (2023). Data should include not only all size bins of PNSD, but also particulate matter mass (PM_{10}, $PM_{2.5}$), gaseous pollutants (NO_2, NO, SO_2, O_3, CO) and black carbon (BC) if available. These variables should be included in order to help the interpretation of the results, since they can be related to main sources.

To start the process, a comma separated values (.csv) file has to be prepared, in which data/time values are provided in the first column and the pairs of data values and related uncertainties are provided for each variable until all of the variables have been included. The first variable would be particle number concentration, then all the size bins, and finally ancillary pollutants.

PMF requires individual uncertainty estimates for each data value. The uncertainty of PNC must be three times the concentration, since it is the total variable. To calculate the uncertainties of the size bins (s_{ij}), a methodology established by Ogulei et al. (2007), Squizzato et al. (2019) and Hopke et al. (2024) can be followed in Equation 1:

$$s_{ij} = \alpha_{ij} + C_3 \cdot n_{ij} \quad (1)$$

where:

$$\alpha_{ij} = 0.01\left(n_{ij} + \bar{n}_{ij}\right)$$

n_{ij} is the concentration of sample i in size bin column j

$\bar{n}_{ij}$ is the arithmetic mean of concentration in size bin j

C_3 is a constant determined by trial-and-error testing values between 0.001 and 0.15.

The lowest and highest bins of the PNSD have been reported to increase the measurement error (Wiedensohler et al., 2018). Consequently, uncertainties for the 3% lowest and 3% highest size bins

are multiplied by a factor of 2, and by a factor of 1.5 for the subsequent 3% lower and 3% higher size bins (Rivas et al., 2019).

Uncertainties for the ancillary pollutants are calculated following the methodology established by Polissar et al. (1998). An additional uncertainty *K* is applied to all the variables.

The program reads in a control file that is modified for the specific data set and the stage of the analysis. A step-by-step set of instructions is provided in the supplemental material files of Hopke et al. (2023). The initial step is to choose the number of factors (sources) to obtain and to execute the base run in which the number of random starts is specified by the number of tasks. Each solution provides an objective value *Q*, and the lowest value is typically explored to determine the utility of this solution. The residuals (difference between the measured and modelled values for a given measured variable) need to be plotted to examine if the given number of factors has provided an adequate fit to the data. Then, factor profiles and contributions that are obtained should be plotted to explore their physical interpretability. If the results are not consistent, PMF should be run again with a different number of factors.

Once the number of factors has been determined and the related base case solution has been selected, the displacement (DISP) analysis should be run. This calculation assesses the amount of rotational displacement that exists in each preselected element of each profile for a very small change in the *Q* value. This will give the minimum and maximum DISP results, and these values can then be plotted along with the base case results.

The selection of the best solution is chosen based on the accepted criteria and guidelines (Belis et al., 2019; Hopke et al., 2023), considering: (i) scaled residuals approximately randomly distributed between -3 and 3, (ii) a Q_{true}/Q_{exp} ratio close to 1, (iii) profile uncertainties determined by the displacement (DISP) method, and (iv) the provision of the most physically meaningful profiles and temporal behaviours.

To support the identification of the sources, the contributions of each factor to the variance of the co-located ancillary pollutants, daily patterns, seasonality and polar plots can be evaluated, and sources have to be identified using existing literature.

Primary pollutants and the particle number size distributions of primary particles can be affected by dispersion, which can result in additional covariance. The process is essentially related to the available air volume in which the pollutants can be mixed. This can be assessed in the first

approximation by the mixing layer height *MLH* and wind speed (WS). The dispersion effect can be corrected by normalizing the input dataset with the ventilation coefficient (*VC*; Dai et al., 2021) in Equation 2:

$$\mathrm{VC}_i = \mathrm{MLH}_i \times u_i, \quad (2)$$

where u_i is the mean wind speed obtained by vectorial averaging for the observation *i*. In Equation 3, the concentration data can be multiplied by the ratio of VC_i and its overall mean value $\overline{VC}$:

$$C_{Vi} = C_i \times \frac{\mathrm{VC}_i}{\overline{\mathrm{VC}}}. \quad (3)$$

After completing the PMF analysis on the corrected dataset, the derived source contributions are to be divided by the respective *VC* ratios to obtain the real contributions. The meteorological variables may affect secondary pollutants and particles in a more complex way. Therefore, it can be advantageous to perform independent PMF modelling both with and without dispersion correction (Vörösmarty et al., 2024). The modelling results can be compared and interpreted together.

3.3. Overview of UFP-PNSD source apportionment studies in Europe

Garcia-Marlès et al. (2024b) analysed datasets in urban Europe to identify and quantify sources contributing to UFP-PNSD using the receptor model PMF, and they also evaluated long-term trends of the source contributions. These datasets were compiled and used with other purposes in previous studies by Trechera et al. (2023), Liu et al. (2023) and Garcia-Marlès et al. (2024a).

3.3.1. Monitoring sites and methodology

The study is based on 24 UFP-PNSD datasets from the period 2009–2019 covering from 3 up to 11 years of data. Data were compiled by the RI-URBANS project and supplied from advanced air quality monitoring networks and research supersites (such as those from ACTRIS). These include (Figure 7 and Table 1):

- Fourteen urban background (UB) sites covering most of Europe: Antwerp (ANT_UB), Athens (ATH_UB), Barcelona (BCN_UB), Budapest (BUD_UB), Dresden (DRE_UB), Granada (GRA_UB), Helsinki (HEL_UB), Lecce (LEC_UB), Leipzig (LEI_UB), London (LND_UB), Madrid (MAD_UB), Mülheim (MUL_UB), Zurich (ZUR_UB), and Rochester (ROC_UB) in New York State in USA.
- Five traffic (TR) sites in Central (C), West (W) and North (N) Europe: Dresden (DRE_TR), Helsinki (HEL_TR), Leipzig (LEI_TR), London (LND_TR) and Stockholm (STO_TR).

- Four suburban background (SUB) sites: Athens (ATH_SUB), Lille (LIL_SUB), Paris (PAR_SUB) and Prague (PRA_SUB).
- One regional background (RB) site in the Po Valley in Italy (Ispra, IPR_RB), which was included because no datasets could be obtained from urban areas in the Po Valley, and this is a pollution hotspot in Europe, where most of the PM pollution has a regional origin.

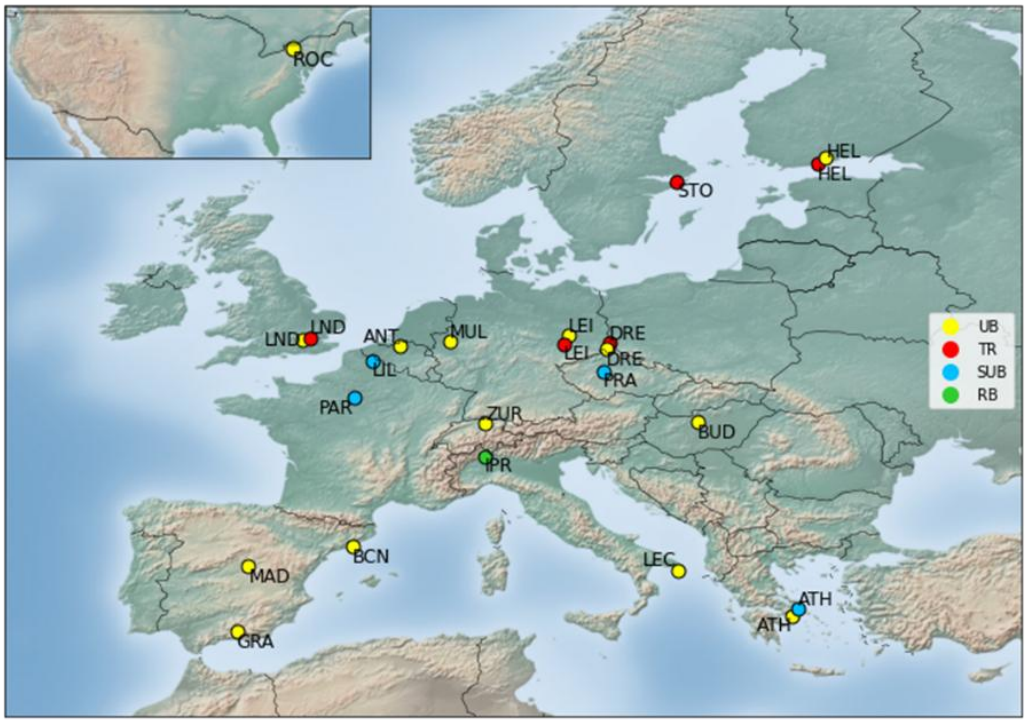

Figure 7. *Location of the cities supplying data on particle number concentrations and size distributions for the study and the type of station. UB, Urban background; TR, Traffic; SUB, Suburban background; RB, Regional background. Adopted from Garcia-Marlès et al. (2024b).*

The data collected from 24 sites were located in 18 European and one USA cities, with different climate and urban structure patterns, UFP concentrations and sources. Data were provided as hourly means of PNSD for this study. The instrumentation used for measuring UFP-PNSD at the different stations is reported in Table 1. The period was selected to obtain relatively recent data without the effect of the decrease of pollution due to the COVID-19 lockdown-associated measures, which were variable across urban Europe and globally (Salma et al., 2020; Dinoi et al., 2021; Eleftheriadis et al., 2021; Petit et al., 2021; Putaud et al., 2021 and 2023).

Table 1. List of air quality sites supplying UFP-PNSD datasets to this study with location, type of environment, period of study, particle size range and equipment used in the study. UB, Urban Background; TR, Traffic; SUB, Suburban Background; RB, Regional Background; Alt., Altitude; SMPS, Scanning Mobility Particle Sizer; DMPS, Differential Mobility Particle Sizer; TSMPS, Twin Scanning Mobility Particle Sizer; TDMPS, Twin Differential Mobility Particle Sizer; CPC, Condensation Particle Counter; TRO, TROPOS; LDMA, long DMA; VDMA, Vienna type DMA; AIRM, Airmodus. Adopted from Garcia-Marlès et al. (2024b).

City (Country)	Station Name	Coordinates (Alt., m a.s.l.)	Acronym	Period	Range	Equipment
Antwerp (BE)	Borgerhout	51.21N, 4.43E (10)	ANT_UB	2017-2019	10-808	SMPS Grimm C5420 L-DMA
Athens (GR)	Thissio	38.00N, 23.72E (110)	ATH_UB	2015-2019	10-470	SMPS TSI 3034
Barcelona (ES)	Palau Reial	41.39N, 2.13E (80)	BCN_UB	2013-2019	12-478	SMPS TSI 3080, CPC TSI 3772
Budapest (HU)	BpART Lab	47.48N, 19.06E (115)	BUD_UB	2009-2019	11-816	DMPS, CPC TSI 3775
Dresden (DE)	Winckelmann Str.	51.04N, 13.73E (120)	DRE_UB	2010-2019	10-800	TRO-TSMPS VDMA 28, CPC TSI 3772
Granada (ES)	UGR	37.16N, 3.61 W (680)	GRA_UB	2017-2019	11-496	SMPS TSI 3082, CPC TSI 3772
Helsinki (FI)	SMEAR III	60.12N, 24.58E (26)	HEL_UB	2009-2019	10-708	TDMPS Hauke-DMA, CPC TSI
Lecce (IT)	ECO Observatory	40.20 N, 18.07 E (50)	LEC_UB	2015-2019	10-800	TRO-SMPS VDMA, CPC TSI 3772
Leipzig (DE)	TROPOS	51.35 N, 12.43 E (113)	LEI_UB	2009-2019	10-800	TRO-TDMPS VDMA, CPC TSI 3025/3010
London (GB)	North Kensington	51.52 N, 0.21 W (27)	LND_UB	2011-2018	17-604	SMPS TSI 3080, CPC TSI 3775 LDMA
Madrid (ES)	CIEMAT-Moncloa	40.45 N, 3.73 W (669)	MAD_UB	2013-2019	15-661	SMPS TSI 3080L, CPC TSI 3775
Mülheim (DE)	Mülheim-Styrum	51.45 N, 6.87 E (39)	MUL_UB	2009-2019	14-496	SMPS TSI 3080, CPC TSI 3772
Rochester NY (US)	NYS DEC	43.15 N, 77.55 W (137)	ROC_UB	2011-2019	12-470	SMPS TSI 3071, CPC TSI 3010
Zurich (CH)	Kaserne	47.38 N, 8.53 E (410)	ZUR_UB	2015-2019	17-478	SMPS TSI 3034, Nafion dryer
Dresden (DE)	North	51.07 N, 13.74 E (116)	DRE_TR	2009-2019	10-800	TRO-TSMPS VDMA, CPC TSI 3025/3010
Helsinki (FI)	Mäkelänkatu	60.19 N, 24.95 E (26)	HEL_TR	2015-2019	11-800	UHEL DMPS VDMA, CPC AIRM A20
Leipzig (DE)	Mitte	51.34 N, 12.38 E (111)	LEI_TR	2010-2019	10-800	TRO-TDMPS VDMA, CPC TSI 3025/3010
London (GB)	Marylebone Rd	51.52 N, 0.15 W (35)	LND_TR	2010-2019	17-604	SMPS TSI 3080, CPC TSI 3775 LDMA
Stockholm (SE)	Hornsgatan	59.32 N, 18.05 E (20)	STO_TR	2012-2018	10-410	DMPS homemade, CPC TSI 3010/3775
Athens (GR)	Demokritos	37.99 N, 23.82 E (270)	ATH_SUB	2010-2019	10-550	SMPS TSI 3080, CPC TSI 3772
Lille (FR)	Villeneuve d'Ascq	50.61 N, 3.14 E (70)	LIL_SUB	2017-2019	20-496	SMPS TSI 3082, CPC TSI 3750
Paris (FR)	SIRTA	48.71 N, 2.16 E (162)	PAR_SUB	2013-2019	11-800	SMPS GRIMM 5416, OPC GRIMM
Prague (CZ)	Suchdol	50.13 N, 14.38 E (277)	PRA_SUB	2012-2019	10-475	SMPS TSI 3034 TRO rebuilt
Ispra (IT)	JRC	45.80 N, 8.63 E (209)	IPR_RB	2016-2019	10-800	DMPS VDMA, CPC TSI 3010/3772

To perform the source apportionment, PMF was applied following the methodology described in the previous section. The datasets for each site were independently analysed by PMF. PMF was run multiple times for different numbers of factors (sources), from 3 to 7 factors, and the number of factors was finally determined by examining the results and choosing the best solution. Then, the results were plotted, and sources were identified using existing literature.

At some sites, nucleated particles from photochemical processes and emitted from road traffic sources were not distinguished by PMF due to their similar PNSDs. A methodology developed by Rodríguez and Cuevas (2007) and Rivas et al. (2019) was used to separate them, using NO_X and BC as proxies for traffic emissions. During morning peaks, NO_X or BC levels were scaled to match traffic-

related PNC. The 10th percentile of the PNC to BC or NO_X ratio during morning rush hours was used as the scaling factor.

After conducting source apportionment, inter-annual trend analysis of the source contributions was conducted using the same methodology as described by Garcia-Marlès et al. (2024a). Monotonic trends over the time were detected using the non-parametric Theil-Sen method (Sen, 1968; Theil, 1992). The magnitude of the trends was quantified by the Theil–Sen slope, which is the median of all the possible slopes between the data pairs, and the statistical significance (*ss*) was also evaluated. These analyses were conducted using the Openair R package (Carslaw and Ropkins, 2012). The individual slopes, expressed as a percentage change per year with their 95% confidence interval, were summarised using random-effects meta-analysis due to the large heterogeneity of the data between the included sites (Chen and Peace, 2013). The mean effect was calculated for each class of site individually (urban, suburban, and traffic sites) as well as globally to provide a comprehensive overview of the results. Meta-analyses were carried out using the Meta R package (Balduzzi et al., 2019).

3.3.2. Results

From 4 to 7 sources were identified at each site. In total, 10 different sources were found for the 24 datasets analysed. Figure 8 shows the relative contributions of the sources at the different sites. Below, the sources identified in the study are described. They were very compatible with the ones identified as dominant in the recent review by Hopke et al. (2022):

- **Traffic-1:** Major size mode around 25–35 nm. Associated to gasoline vehicle emissions, freshly emitted traffic particles or nucleation of diesel particles. Peaks observed during traffic rush hours and minimum values occur on weekends.
- **Traffic-2:** Major size mode around 60–100 nm. Associated to diesel vehicle emissions or coagulation of traffic particles when moving from the sources. Peaks observed during traffic rush hours and minimum values occur on weekends.
- **Mixed traffic**: Major size mode between those of Traffic-1 and Traffic-2, due to a mix of all traffic sources and other sources not related to traffic, such as domestic heating.
- **Traffic-Nucleation:** Major size mode around 10–20 nm. Associated to the nucleation of particles generated during dilution of diesel exhaust emissions. Diurnal trends are similar to those described for the aforementioned traffic sources.

- **Photonucleation:** Major size mode around 10–20 nm. A midday peak is found when high photochemical activity leads to new particle formation events.
- **Urban background:** Major size mode around 100–180 nm. It is influenced by traffic emissions, exhibiting similar diurnal trends to those of the traffic sources.
- **Summer regional:** Typically, it shows a bimodal distribution with a primary size mode above 150 nm, reaching its maximum during summer and at midday.
- **Winter regional**: It shows a distribution similar to the previous one, but with the maximum occurring during winter and at night.
- **Domestic heating**: Major size mode around 100 nm. It is associated with the combustion of fuels, and peaks during the night and winter.
- **Long distance transport:** Multimodal distribution with a primary mode around 300 nm. Associated to dust from, e.g., deserts, traffic, and forest fires.

The results show that road traffic is the major contributor to UFP/PNC in urban Europe. The sum of the 2 to 4 traffic contributions (Traffic-1, Traffic-2, Mixed traffic and Traffic-Nucleation) reached the highest source contribution to UFP/PNC in all cities, with 70–88% of the UB average UFP/PNC concentrations in 9 of the 14 cities analysed, and 47–61% in the remaining 5 (Figure 9). Following traffic, Photonucleation (new particle formation mostly at regional scale) was contributing with 31 and 24% in BCN_UB and DRE_UB (and 4–18% in the remaining 10 UB sites that this source was identified). Continuing with the UB sites, lower contributions were obtained for Summer regional (0–16%), Winter regional (0–7%) and Urban background (0–14%). The long-range transport (desert dust, forest fires, etc.) was only identified in BCN_UB and with very low contributions.

As it could be expected, at TR sites the traffic contribution was the main source of UFP/PNC, with 77–95% share at the five study sites, with much lower contributions of other sources. It is important to note that the Traffic-Nucleation was more relevant in these TR sites than in the UB ones. This nucleation might have arisen from gasoline emissions but mainly from the nucleation of SVOCs escaping the diesel particle filters (DPFs) (Harrison et al., 2011; Damayanti et al., 2023). These nucleated particles grow very fast as the distance from the traffic source increases. However, it is also very relevant to note that in many cases, the PMF analysis yielded a mixed Traffic-Nucleation and Photonucleation source contribution with major peaks at traffic rush hours and at midday, and these had to be split based on the NO_2 or BC tracer method (Rodriguez and Cuevas, 2007). In these cases, the error in quantifying source contributions might have been higher. Furthermore, in

HEL_TR, the PMF analysis yielded a source profile with regional background and traffic patterns that was not possible to be split.

At the SUB and RB sites, traffic was also the major contributor to average UFP/PNC, with 22–77% share.

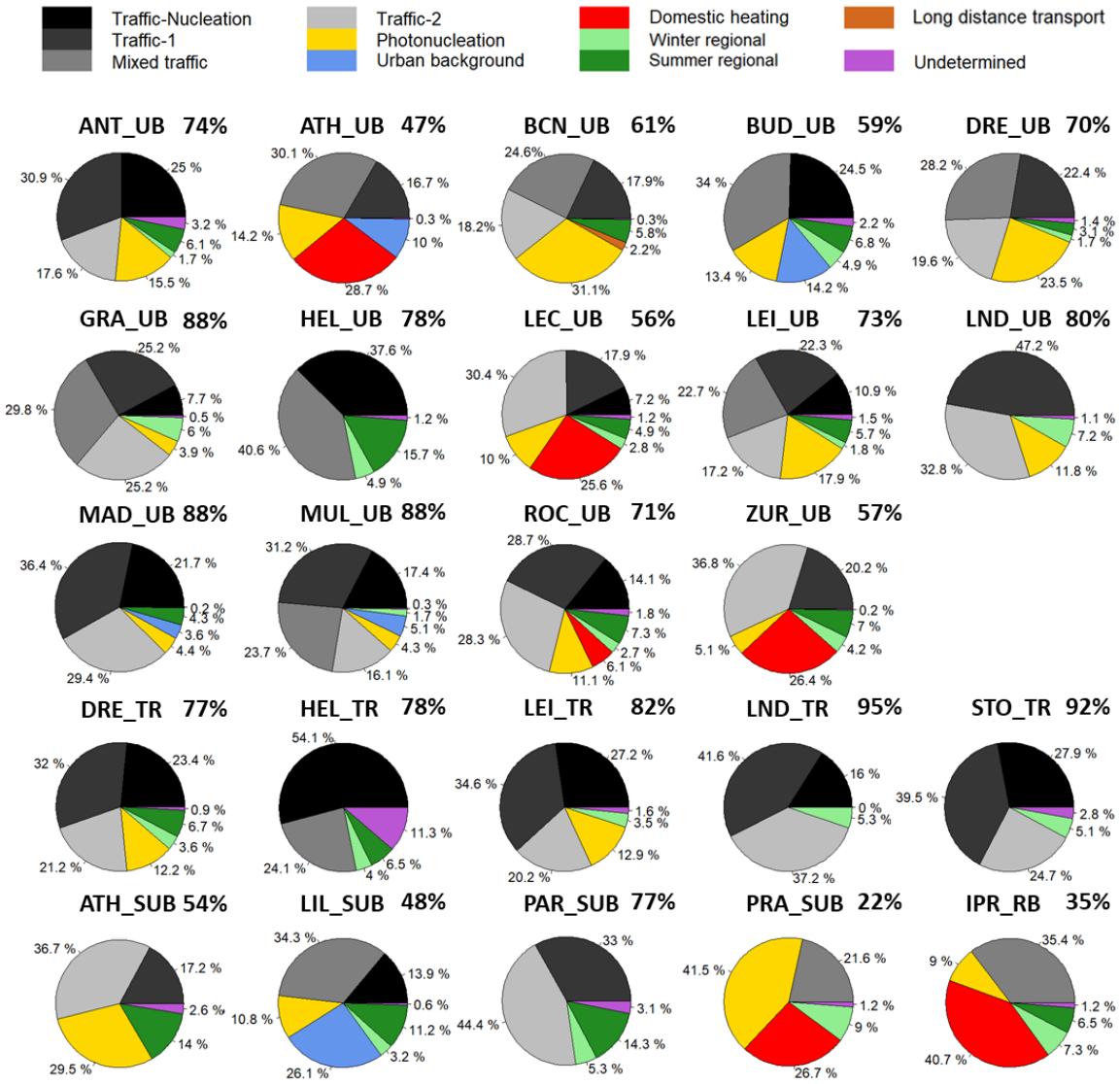

Figure 8. *Average source contributions (%) to PNCs obtained for each study site. Next to the site name, the total traffic contribution (%) is presented. Adopted from Garcia-Marlès et al. (2024b).*

3.4. Recommendations for UFP-PNSD source apportionment

3.4.1. Source apportionment of UFP-PNSD

Recommendations for UFP-PNSD are the following:

- Check carefully the quality of the data sets from particle number size distribution (PNSD) measurement, by identifying anomalous data with extremely high or low values, detecting anomalous jumps in the PNSD, among others. Clean the dataset of possible spurious data.
- Be sure that the lower size limit value starts at least at 10 nm, and that recommendations from CEN and ACTRIS are followed (CEN, 2020, 2024; ACTRIS, 2021). See also RI-URBANS ST1 guidance for UFP-PNSD measurements in https://riurbans.eu/project/#service-tools.
- Use the Positive Matrix Factorization (PMF) algorithm as a receptor model.
- Use ancillary co-pollutants measured in-situ and simultaneously (NO_2, NO, SO_2, CO, BC, O_3, PM_x) and include these in the PMF.
- Collect also meteorological data, especially wind direction and speed.
- Use hourly data for the urban background and higher resolution if measurements are done around specific sources (e.g., airports, harbours).
- Source apportionment of UFP-PNSD for large datasets may be performed by PMF using the tool developed by Hopke et al. (2023).
- PMF requires individual uncertainty estimates for each data value. The uncertainty of PNC must be three times the concentration since it is the total variable. To calculate the uncertainties of the size bins, a methodology established by Ogulei et al. (2007), Squizzato et al. (2019) and Hopke et al. (2024) is recommended.
- PMF has to be run multiple times with different number of factors. The selection of the best solution is chosen based on the accepted criteria and guidelines (Belis et al., 2019; Hopke et al., 2023), considering: (i) scaled residuals approximately randomly distributed between -3 and 3, (ii) a Q_{true}/Q_{exp} ratio close to 1, (iii) profile uncertainties determined by the displacement (DISP) method, and (iv) the provision of the most physically meaningful profiles and temporal behaviours.

3.4.2. Main findings on source apportionment of UFP-PNSD

- The results show that road traffic is the major contributor to UFP/PNC in urban Europe.
- Four traffic contributions were identified (traffic from diesel vehicles, traffic from gasoline

vehicles, traffic nucleation, and mixed urban traffic). The sum of these reaches the highest source contribution to UFP/PNC in all cities, with 70–90% of the UB average UFP/PNC concentrations in 8 of the 12 cities analysed, and 56–62% in the remaining four.

- In the UB sites, following traffic, photonucleation (new particle formation mostly at regional scale) is contributing with 31 and 24% in BCN_UB and DRE_UB (probably due to enhanced shipping and regional coal fired power plant emissions, respectively); and domestic heating, with 26% in both ZUR_UB and LEC_UB. Lower contributions were obtained for regional summer (0–16%), regional winter (nitrate 0–10%) and urban background (14% in BUD_UB) while long-distance transport (e.g., desert dust, forest fires) was only identified in BCN_UB and with very low contributions.
- As could be expected at TR sites, the traffic contribution was the main source of UFP/PNC, with 79–85% at the four study sites, with much lower contributions of other sources. It is important to note that the traffic nucleation is more relevant in the TR sites than in the UB ones. As stated in the trend analysis section, this nucleation might arise from gasoline emissions but mainly from the nucleation of SVOCs escaping the DPFs in diesel vehicles. These nucleated particles grow very fast as the distance from the traffic source increases.
- At the SUB sites, traffic is also the major contributor to average UFP/PNC, with 68–77% share.
- To abate UFP pollution in urban areas, emissions from road traffic should be targeted, although contributions from photochemical nucleation from power plants' plumes, harbours, airports, or domestic sources might also contribute to the increase of urban UFP.

4. OXIDATIVE POTENTIAL OF PM SOURCE APPORTIONMENT

4.1. Context

The capacity of aerosols to generate reactive oxygen species (ROS) in vivo has recently been introduced as a pivotal indicator of PM biological mechanism with direct implications for oxidative stress and cellular damage called oxidative potential (OP) of PM (Li et al., 2008; Lodovici and Bigagli, 2011; Mudway et al., 2020; Ayres et al., 2008; Akhtar et al., 2010; Leni et al., 2020). In this document, the oxidative potential is only related to particulate matter (even if gas may also affect it), and the oxidative potential of PM is abbreviated as OP here.

The relationship between PM chemical components and OP levels may indicate which components are the most prone to generating ROS (Calas et al., 2019; Godri et al., 2011; Crobeddu et al., 2017; Calas et al., 2018). However, this research pathway struggles with the co-variation between measured and unmeasured PM components (Calas et al., 2018; Weber et al., 2018), with detailed chemical characterization being very costly and a very large number of organic species being currently not determined in PM. An alternative approach is to examine the association between OP and sources of PM obtained using the so-called "receptor models" such as chemical mass balance (CMB), PMF, or principal component analysis (PCA). PMF is the most popular method for its ability to quantify PM source contributions without extensive prior information on specific sources at the site studied (Paatero and Tappert, 1994; Paatero and Hopke, 2009; Rusanen et al., 2024; Via et al., 2022).

After this first step, it is possible to estimate the redox activity of receptor-model-derived PM sources (Bates et al., 2015; Weber et al., 2018, Deng et al., 2022; Shangguan et al., 2022). Generally, this is achieved by multiple linear regression analyses (MLR) to characterize the relationship between OP activities (nmol min^{-1} m^{-3}) and PM source contributions (μg m^{-3}). This approach provides the OP activities attributed to each microgram of each source (nmol min^{-1} μg for a source), labelled "intrinsic OP", which can be used to calculate the contribution of each source for each observation day. This method of attribution of OP to sources does not require to know the very detailed chemistry of the samples, but only the specific tracers of each of the sources. With such an approach, designing the dataset such that sufficient source variation is included is crucial. Generally, at least one year of equally spaced 24 h filters every 3–4 days for $PM_{2.5}$ or PM_{10} is ideal. The proper set of tracers also needs to be determined and analysed. Recommendations on all these points were provided by the EU FAIRMODE Working Group[1]. Insufficient variability in the contributions of sources can lead both to issues in resolving PM's sources via PMF as well as in attributing OP to its sources via MLR. Overall, independent of the chosen regression model, the quality of the PMF-derived sources (i.e., time series) governs the quality of the OP source apportionment. However, there is a need for more research to improve these methods and overcome some issues in order to reduce the uncertainties of the results.

1 https://fairmode.jrc.ec.europa.eu/activity/ct1

4.2. Selection of the regression model

Particularly, numerous regression models can be used for such OP SA, with MLR fitted by ordinary least squares (OLS) being the most common regression technique (Bates et al., 2015; Deng et al., 2022; Shangguan et al., 2022; Weber et al., 2018). Additionally, weighted least squares can be used to introduce a weighting term, generally using the OP analysis uncertainties to consider the measurement uncertainties of the OP assays (Borlaza et al., 2021; Daellenbach et al., 2020; Dominutti et al., 2023; Fadel et al., 2023; in't Veld et al., 2023; Weber et al., 2021). Two critical assumptions in regression analysis are that (i) there is little collinearity between independent variables (the PM_{10} sources in this study) and (ii) the variance of the regression residuals is constant (called "homoscedasticity"). Collinearity occurs when one or more of the independent variables is close to a linear combination of the other independent variables. Heteroscedasticity occurs when the variance of regression residuals is not constant but varies for different values of the dependent variable. In this case, the estimated standard errors of the regression coefficients are not reliable. These assumptions should be tested in different ways. Dinh et al. (2024) proposed a workflow to select the best model of inversion regarding the dataset properties (Figure 9).

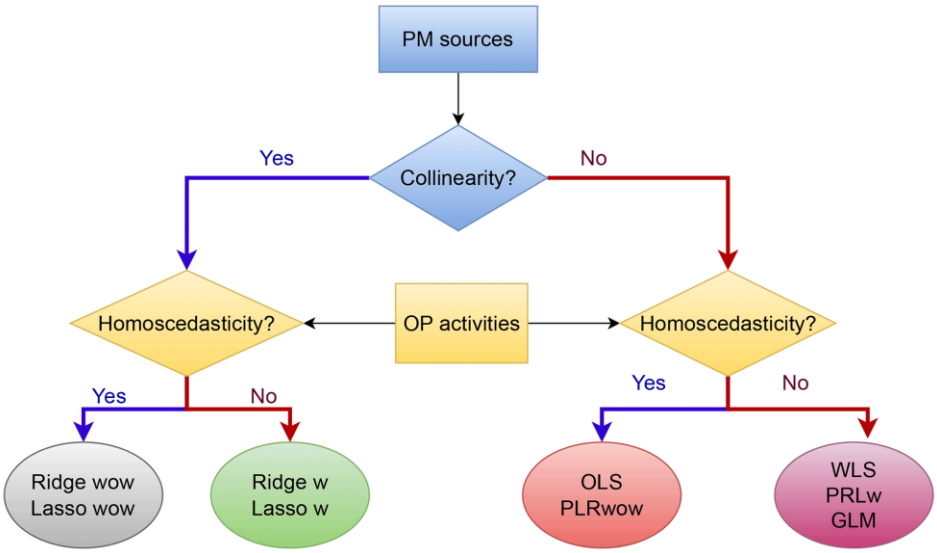

Figure 9. *Workflow in model selection considering the data characteristics. Adopted from Dinh et al. (2024).*

4.3. Accuracy of the modelling and recommendations

Several challenges exist in the source apportionment of OP of PM. One is overfitting, i.e., including too many PM sources as predictors in the multilinear regression model for explaining OP, that can

lead to highly uncertain results and even non-physical intrinsic OP (i.e., negative). The effect of overfitting and the model's performance in general can be accessed via cross-validation, i.e., leaving data out that are only used to check the predictive power of the model. Such risk of overfitting can be handled in different ways. Some studies exclude sources with negative intrinsic OP, assuming that negative OP activities are geochemically not meaningful (Bates et al., 2018; Weber et al., 2018). Others group predictors to reduce collinearity (Camman et al., 2024; Cheung et al., 2024) or select sequentially (forward or backward) a subset of predictors based on information criteria (Daellenbach et al., 2020; Bhattu et al., 2024).

Finally, interactions between PM components affecting their OP activity have been postulated, e.g., solubility of metals or interaction with biological particles (Samake et al., 2017). Non-linear models such as multilayer perceptron (MLP) or Random Forest (RF) (Borlaza et al., 2021; Elangasinghe et al., 2014) were used in attempts to capture such processes. However, these approaches require larger datasets than the ones typically used with linear models, even larger than most existing databases so far. As a rule of thumb, the number of OP data points should be at least 15 times the number of predictors. Cross-validation for non-linear models is even more important than for the linear multilinear regression models and requires even more data. In addition, these models based on machine learning do not provide estimates of intrinsic OP (nmol min^{-1} μg^{-1}) but only the importance of each PM_{10} source to the OP prediction. This is a major drawback, since the intrinsic OP of sources is a prerequisite for the modelling effort of OP with chemical transport models (CTM) (Daellenbach et al., 2020). However, RF and MLP could be useful for OP prediction in the case of larger datasets generated by online instruments.

4.4. Overview of OP of PM source apportionment studies in Europe

Despite suggestions that OP of PM plays a significant role in the acute health impacts of PM, the precise links remain unclear. Investigations into which components of PM exhibit oxidative activity have produced contrasting findings, leaving much yet to be understood about the sources of PM that may influence OP. Consequently, there is growing interest in exploring the health risks associated with PM exposure by examining OP, particularly in the European context. Here we report on primary findings collected from studies conducted in the region applying source apportionment and MLR models.

A study in Spain (In 't Veld et al., 2023) included the evaluation of PM_{10}, $PM_{2.5}$, and PM_1 samples collected roughly every four days at an urban background site and a rural background site. This is one of the few studies in Europe evaluating the OP at three different PM sizes over one year and also comparing two different site typologies. The assessment of the chemical composition of PM samples allows the application of source apportionment using PMF to identify the main PM sources. The OP^{DTT} and OP^{AA} of PM were determined. OP^{DTT} and OP^{AA} are OP measurements related to the use of different probes (lung antioxidant or surrogate), DTT (1,4-dithiothreitol) and AA (ascorbic acid) assays, respectively. More information on the selection of the assay can be found in the RI-URBANS Service Tool ST4 (https://riurbans.eu/project/#service-tools). Finally, to link the sources with the measured OP, MLR models were applied to the datasets. The findings revealed that in Barcelona, OP of PM_{10} was notably higher compared to that of $PM_{2.5}$ and PM_1. Conversely, at the rural site, the results across all PM sizes were within a similar range but notably lower than those observed in the urban site. In the urban area, various anthropogenic sources emerged as the primary influencers of OP in PM_{10} (including combustion, road dust, heavy oil, and OC-rich sources) and $PM_{2.5}$ (road dust and combustion). In contrast, the rural site showed no distinct factors influencing OP evolution, which likely accounts for the absence of a notable difference in OP among PM_{10}, $PM_{2.5}$, and PM_1. This study underscored the importance of size fractions in determining OP, depending on the environmental context. In urban settings, OP is influenced by both PM_{10} and PM_1 size fractions, whereas in rural environments, only the PM_1 fraction is significant (in 't Veld et al., 2023).

In the study of Daellenbach et al. (2020), the authors used field observations and air-quality modelling to assess the primary and secondary origins of PM and OP across Europe. The main findings were in line with the results observed in Switzerland (Grange et al., 2022), which reveal that the mass concentration of PM is predominantly influenced by secondary inorganic components, crustal material, and secondary biogenic organic aerosols. In contrast, anthropogenic sources, notably fine-mode secondary organic aerosols from residential biomass burning and coarse-mode metals from vehicular non-exhaust emissions, are the primary contributors to OP activities.

Similar results were also obtained from the OP measurements conducted using two distinct acellular assays (OP^{DTT} and OP^{AA}) on PM_{10} samples collected over a yearly time series from 14 diverse locations across France from 2013 to 2018 (Figure 10). Distinct positive redox activity towards the OP^{DTT} assay was observed for primary road traffic, biomass burning, dust, MSA-rich, and primary

biogenic sources. Conversely, biomass burning and road traffic sources exhibited significant activity solely for the OP^{AA} assay. The daily median contribution of each source to total OP^{DTT} emphasized the predominant influence of the primary road traffic source. Both biomass burning and road traffic sources contributed equally to the observed OP^{AA} (Weber et al., 2021). The OP was found to be comparable between the French datasets and those obtained in Switzerland through the same sampling and laboratory procedures.

Consequently, residential biomass burning and road traffic stand out as the primary targets for prioritization in significantly reducing OP levels in Western Europe. In addition, these results suggest that strategies focused solely on reducing the mass concentrations of PM may not effectively decrease OP levels. If the oxidative potential is closely linked to significant health impacts, targeting specific sources of PM rather than overall PM mass could be a more efficient mitigation approach (Daellenbach et al., 2020; Weber et al., 2021).

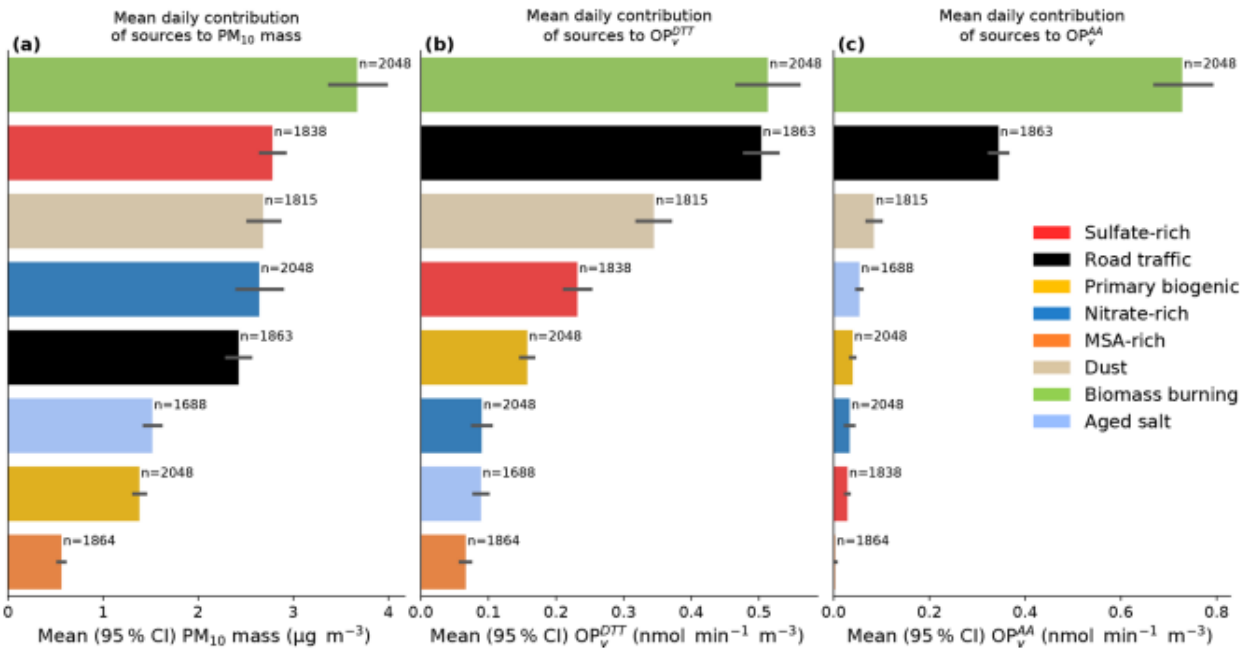

Figure 10. *Median daily contribution of the sources to the $OP^{AA}v$, the $OP^{DTT}v$ and the PM mass. The bars represent the mean, and the error bars represent the 95 % confidence interval of the median.*

A recent study (Dominutti et al., 2023) explored five distinct acellular OP assays and their sensitivity to the chemical composition of atmospheric PM_{10} and its emission sources collected at an urban alpine city in France. This included the assessment of well-established assays like AA, DTT, and DCFH (2,7-dichlorodihydrofluorescein), alongside novel assays such as Ferric-Xylenol Orange (FOX) and

direct ROS quantification via ●OH. The main findings underscored the significant influence of seasonality on source contributions and OP activities. In winter, when anthropogenic emissions dominate, all OP assays exhibited strong agreement. Conversely, in warmer months, with reduced anthropogenic influence, biogenic and secondary organic-related aerosols exerted a greater impact. Additionally, the study observed varying sensitivities of each OP assay to PM_{10} sources, likely reflecting differences in chemical composition and processes (Dominutti et al., 2023, Figure 11).

The results also emphasize the necessity of employing multiple OP assays to capture diverse sensitivities to redox-active species, providing deeper insights into the intrinsic capacity of PM sources to induce OP reactions. Given the heterogeneity of sources identified by different OP assays for a given ambient PM exposure, the selection of a single or combination of OP method(s) should be carefully considered as part of the assessment strategy. Such informed choices can provide valuable source-related information guiding targeted reduction policies (Dominutti et al., 2023).

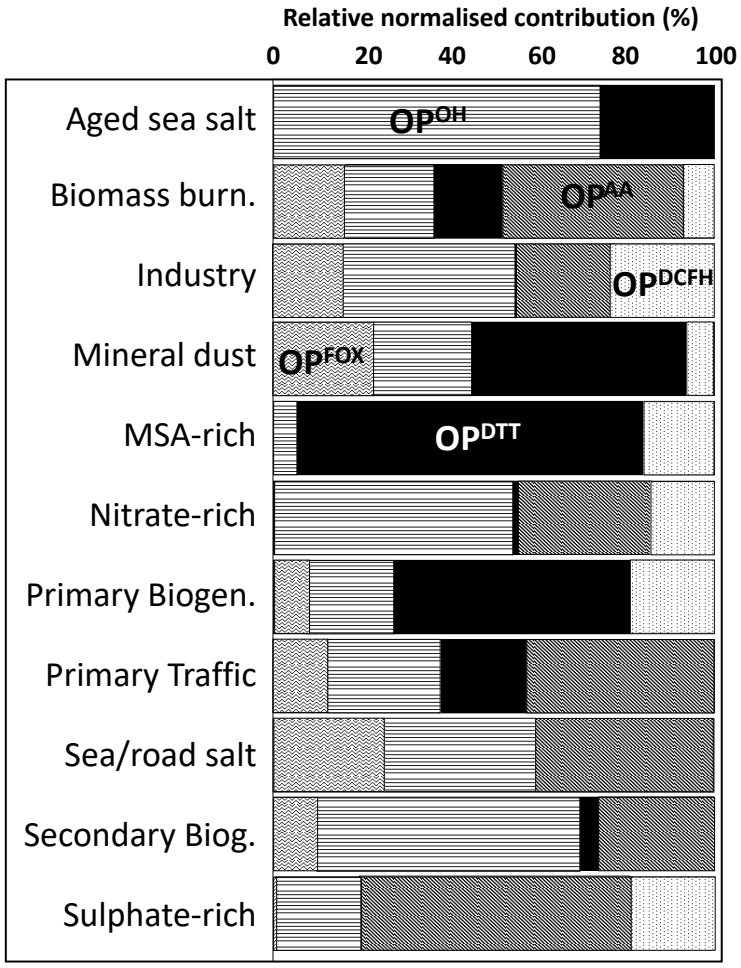

Figure 11. *OP sensitivity contribution of each PM source. Relative normalised contribution of OP assays to the PM_{10} sources. Colours represent each OP test evaluated. Adopted from Dominutti et al. (2023).*

4.5. Recommendations for OP source apportionment

The current state of the art of the source apportionment (SA) of oxidative potential (OP) already provides useful results to evaluate what are the main sources of OP, e.g., the sources of sanitary interest that are potentially detrimental for human health. The OP results also begin to be used in chemical transport models (CTM) for large sale studies over Europe and the USA, and an increasing number of models now include OP for forecasting, retrospective studies, and future scenarios. However, there are still many pathways for investigations to improve these methods of attribution. It is recommended:

- Using the most widely used OP measurement protocols until the harmonisation of OP analysis (see RI-URBANS Service Tool ST4 on OP of PM)[2].
- Analysing the speciation of PM using a complete list of PM source tracers including inorganic and organic compounds/elements (see RI-URBANS Service Tool ST3 on PM speciation) [1].
- Generally, at least 1 year of equally spaced 24h filters every 3–4 days for $PM_{2.5}$ or PM_{10} is adequate.
- Implement a detailed SA, using positive matrix factorization (PMF) or other receptor models ensuring a robust solution, otherwise the OP SA will be uncertain (see RI-URBANS Service Tool ST10 on SA of PM[1]).
- Implement a post multilinear regression (MLR) analysis, by combining OP and PMF outputs of the samples, to associate OP and source contributions. This approach provides the OP activities attributed to each µg of each source (nmol min^{-1} µg for a source), labelled "intrinsic OP", which can be used to calculate the contribution of each source for each observation day.
- The choice of the model has to be done according to the dataset properties, and two critical assumptions (collinearity and heteroscedasticity) need to be tested to select the best adapted model.

2 The Service Tools are available at https://riurbans.eu/project/#service-tools.

5. VOC SOURCE APPORTIONMENT

5.1. Overview of VOC source apportionment studies in Europe

The literature review on the source apportionment of VOCs in urban and urban background areas showed that, to our knowledge, 18 studies have been performed in Europe. In Table 2, we present these studies as well as additional studies performed in rural areas in Europe. Positive Matrix Factorization model (PMF), using the EPA 5.0 software in general or older versions, was used in the majority of the papers to perform the source apportionment either on seasonal basis when long term data is available, or on specific campaign's data. The EPA software is the most suitable as it does not require previous knowledge on the source composition profile, and it has built-in bootstrapping and error estimations for the model. This section focuses on the summary of these studies and highlights their conclusions as follows:

- The majority of the studies used online gas chromatograph with flame ionization detector (GC-FID), and proton transfer reaction mass spectrometry (PTR-MS), using either a quadrupole or time of flight mass detector to measure ambient VOC concentrations.
    - The online GC-FID allows the measurement of C_2–C_{11} NMHC covering alkanes, alkenes including isoprene, alkynes, and aromatics on hourly basis in general.
    - The PTR-MS allows the measurement of mainly aromatics, oxygenated VOCs, sum of monoterpenes, with high time resolution.
- A variety of factors were identified in the urban environment. In all articles, a total of around 100 unique VOCs were measured. The identified sources are described with their common tracers/markers below. Note that some sources are only identified in some specific seasons, like wood-burning in winter.
    - Natural gas source was mostly identified by high contributions of ethane and propane, with minor contributions from butane.
    - Wood-burning source was traced by acetonitrile, acetylene, ethylene, and benzene.
    - Biogenic source was identified by isoprene and its oxidation products (Methyl Vinyl Ketone (MVK) and Methacrolein (MACR)). Although isoprene has a biogenic origin, its anthropogenic origin is rarely described. The addition of monoterpenes can potentially aid in identifying its biogenic origin, although they are often emitted from other vegetation (potentially being

identified as a separate factor), and also monoterpenes can be emitted from anthropogenic sources.

- Motor vehicle exhaust was characterized by high contributions from C_4–C_5 alkanes, especially butane and pentane, and BTEX (benzene, toluene, ethylbenzene, and xylenes) compounds. The exact tracers highly depend on the type of traffic and engines most commonly used in the urban area, and depending on the VOCs included in the study. The traffic exhaust was either separated or combined with fuel evaporation related to traffic.
- Solvent source markers often had high contributions of OVOCs and aromatics in these studies.
- Some specific industry sources were found, but this highly depended on the type of industry and on which VOCs were used to identify this source.
- Various studies found a secondary source composed of OVOCs mainly, although some studies identified this source as long-lifetime VOCs.

Within RI-URBANS, three source apportionment studies were performed after data collection at two urban/urban background sites with different VOC datasets in Marseille, France (Dufresne, 2022), and Zurich, Switzerland. The Marseille database covered one year and a half of hourly measurements of C_2–C_{16} non-methane hydrocarbons (NMHCs) while the Zurich database covered two-years of hourly measurements of C_2–C_7 NMHCs, monoterpenes, C_2–C_5 oxygenated VOCs (OVOCs), and acetonitrile. Both datasets have been obtained by using online thermal-desorption gas-chromatography flame-ionization-detector (TD-GC-FID) on an hourly basis (Marseille) or 90 minutes (Zurich).

The 5.0 version of the PMF tool from the Environmental Protection Agency (EPA) was used on a seasonal basis for both datasets. The PMF inputs are the measured concentrations and their associated uncertainties. At both sites, the uncertainties estimation followed the ACTRIS guideline (https://www.actris.eu/sites/default/files/inline-files/WP3_D3.17_M42_0.pdf).

For both datasets, some data were missing or below the limit of detection (LOD) and should be replaced since missing values are not accepted by the PMF. Concerning concentrations below the LOD, the concentrations were replaced by the LOD divided by 2 and uncertainties were calculated following the Equation 4:

$$U = \frac{5}{6} \times LOD \qquad (4)$$

Where U is the uncertainty (in µg m^{-3}).

The missing values were replaced with the hourly median of the same month. In this case, the associated uncertainty was the hourly median multiplied by 4. These replaced values had a low impact on the PMF results as the weight given by the PMF to a measurement depends on the uncertainty.

For each season of both datasets, twenty runs were performed with a number of factors varying from 3 to 12. Several parameters were plotted versus the number of factors to determine the best solution following the method from Lee et al. (1999) and Hopke (2000).

Table 2. *Overview of VOC source apportionment studies in Europe (urban and rural sites). Continues on the next page.*

	Reference	Title	Station	Location	Method	Apportionment
European Urban	Borbon et al. (2002)	Characterisation of NMHCs in a French urban atmosphere: overview of the main sources.	Urban	Lille, FR	GC-FID	PCA
	Hellén et al. (2003)	Source contributions of NMHCs in Helsinki using chemical mass balance (CMB) and multivariate (Unmix) receptor models.	Urban	Helsinki, FI	GC-FID GC-MS	CMB Unmix
	Hellén et al. (2006)	Ambient air concentrations, source profiles and source apportionment of 71 different C2-C10 volatile organic compounds in urban and residential areas of Finland.	Urban	Helsinki, FI	GC-FID GC-MS	CMB
	Badol et al. (2008)	Using a source-receptor approach to characterize VOC behaviour in a French urban area influenced by industrial emissions Part I: Study area description, data set acquisition and qualitative data analysis of the data set	Urban	Dunkerque, FR	GC-FID	CMB
	Lanz et al. (2008)	Receptor modelling of C_2 – C_7 hydrocarbon sources at an urban background site in Zurich, Switzerland: changes between 1993 – 1994 and 2005 – 2006.	Urban	Zurich, CH	GC-FID	EPA PMF 5.0
	Gaimoz et al. (2011)	Volatile organic compounds sources in Paris in spring 2007. Part II: Source apportionment using positive matrix factorization.	Urban	Paris, FR	GC-FID PTR-QMS	PMF2
	Hellén et al. (2012)	Importance of isoprene and monoterpenes in urban air in Northern Europe.	Urban	Helsinki, FI	GC-MS	Unmix
	Yurdakul et al. (2013)	Volatile organic compounds in suburban Ankara atmosphere, Turkey: Sources and variability	Urban	Ankara, TR	GC-FID	PMF2

	Reference	Title	Station	Location	Method	Apportionment
	Patokoski et al. 2014	Winter to spring transition and diurnal variation of VOCs in Finland in an urban background site and a rural site.	Urban/rural	Helsinki, FI	PTR-QMS	Unmix
	Baudic et al. (2016)	Seasonal variability and source apportionment of volatile organic compounds (VOCs) in the Paris megacity (France).	Urban	Paris, FR	PTR-QMS GC-FID	EPA PMF 5.0
	Kaltsonoudis et al. (2016)	Temporal variability and sources of VOCs in urban areas of the eastern Mediterranean	Urban	Athens+ Patras, GR	PTR-QMS	PMF
	Thera et al. (2019)	Composition and variability of gaseous organic pollution in the port megacity of Istanbul: source attribution, emission ratios, and inventory evaluation	Urban	Istanbul, TR	PTR-QMS GC-FID	EPA PMF 5.0
	Languille et al. (2020)	Wood burning: A major source of Volatile Organic Compounds during wintertime in the Paris region	Urban	Paris, FR	PTR-QMS	EPA PMF 5.0
	Panopoulou et al. (2021)	Variability and sources of non-methane hydrocarbons at a Mediterranean urban atmosphere: The role of biomass burning and traffic emissions	Urban	Athens, GR	GC-FID	EPA PMF 5.0
	Dufresne (2022)	Sources et déterminants des composés organiques volatils à Marseille	Urban	Marseille, FR	GC-FID	EPA PMF 5.0
	Liakakou et al. (2022)	Variability and sources of NMHCs at a coastal urban location in the Piraeus Port	Urban	Piraeus, GR	GC-FID	PMF
	Leïla Simon, PhD (2023)	Détermination des sources de composés organiques (gazeux et particulaires) en Ile-de-France	Urban	Sirta – Paris, FR	PTR-MS	PMF ME-2
	In 't Veld et al. (2023)	Identification of volatile organic compounds and their sources driving ozone and secondary organic aerosol formation in NE Spain.	Urban Rural	Barcelona, ES NE Spain	PTR-QMS PTR-ToF-MS	EPA PMF 5.0
European Rural	Sauvage et al. (2009)	Long term measurement and source apportionment of non-methane hydrocarbons in three French rural areas	Rural	France	GC-FID	PMF2
	Leuchner et al. (2015)	Can positive matrix factorization help to understand patterns of organic trace gases at the continental Global Atmosphere Watch site Hohenpeissenberg.	Rural	Germany	GC-FID	EPA PMF 3.0
	Debevec et al. (2017)	Origin and variability in volatile organic compounds observed at an Eastern Mediterranean background site (Cyprus)	Rural	Cyprus	PTR-QMS GC-FID	EPA PMF 5.0
	Michoud et al. (2017)	Organic carbon at a remote site of the western Mediterranean Basin: sources and chemistry during the ChArMEx SOP2 field experiment	Rural	Ersa, FR	PTR-ToF-MS GC-FID	EPA PMF 3.0
	Debevec et al. (2021)	Seasonal variation and origins of volatile organic compounds observed during 2 years at a	Rural	Ersa, FR	GC-FID	EPA PMF 5.0

Reference	Title	Station	Location	Method	Apportionment
	western Mediterranean remote background site (Ersa, Cape Corsica)				
Vestenius et al. (2021)	Assessing volatile organic compound sources in a boreal forest using positive matrix factorization (PMF)	Rural	Finland	GC-MS	EPA PMF 5.0
Yáñez-Serrano et al. (2021)	Dynamics of volatile organic compounds in a western Mediterranean oak forest.	Rural	NE Spain	PTR-QMS	EPA PMF 5.0
Hellén et al. (2024)	Shipping and algae emissions have a major impact on ambient air mixing ratios of non-methane hydrocarbons (NMHCs) and methanethiol on Utö Island in the Baltic Sea	Rural	Finland	GC-FID/MS	EPA PMF 5.0

To summarize, the latest two PMF studies at two European urban background sites show some common sources between Marseille and Zurich (like road transport, natural gas, heating/wood burning, and local emissions). One source related to solvent use was identified only in Zurich thanks to OVOC data (Figure 12). Additional sources were identified in Marseille related to industrial sources surrounding the site. Since the two datasets did not cover the same VOCs, having a wide range of VOCs with varying volatility, including intermediate-volatility organic compounds (IVOCs) and both primary (non-methane hydrocarbons, NMHCs) and secondary origins (oxygenated VOCs, OVOCs), is essential. This broader spectrum can aid in identifying the sources and assessing their contribution. Additionally, the measurement of OVOCs is important as it is an indicator of the impact of photochemistry and covers some markers of solvent use emission source.

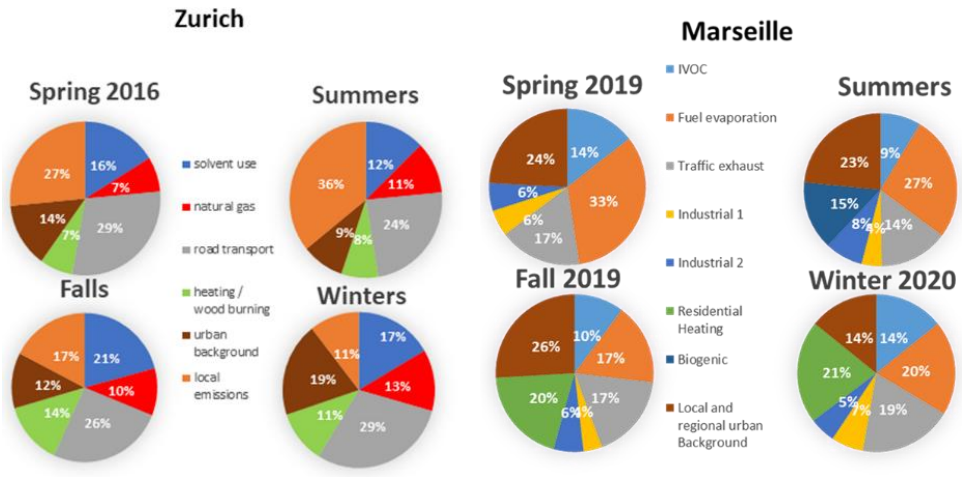

Figure 12. *Source apportionment results at Marseille (Dufresne, 2022) and Zurich.*

The third RI-URBANS study (In 't Veld et al., 2023) was carried out in Barcelona, Spain, using PTR-QMS and PTR-ToF-MS in rural and urban background sites (for several months in summer and winter), using a similar PMF 5.0 approach to the one described for Zurich and Marseille. However, in this case the number of species analysed was lower (11) compared with the studies from Zurich and Marseille. They found 5 major factors contributing to VOCs:

- **Anthropogenic I. Traffic and industry:** Traced by toluene (81% of the total toluene explained by this factor) and C_8 aromatics (67%), with tracers of benzene (25%) and isoprene (19%).
- **Anthropogenic II: Traffic and biomass burning:** Traced by benzene (69%), acetaldehyde (67%), and acetonitrile (36%), as well as various oxidized VOCs (OVOCs), such as MEK (27%), methanol (19%), and C_8 aromatics (19%).
- **Isoprene oxidation:** traced by isoprene (81%) and MVK + MACR (65%), both of which are oxidation products of isoprene.
- **A biogenic source:** At both stations contained only monoterpenes.
- **Long-lifetime VOCs:** A source combining the VOCs with long atmospheric lifetimes traced by various OVOCs, including acetone (71%), methanol (69%), acetonitrile (61%), MEK (40%), MVK + MACR (31%), and acetaldehyde (23%).

All these studies calculated also the individual contributions to the maximum O_3 and SOA formation potentials from the identified sources at Marseille, Zurich, and Barcelona.

5.2. Recommendations for VOCs source apportionment

- VOCs datasets (preferable online) should be obtained following the recommendations of RI-URBANS Service Tool ST5 on VOCs (see https://riurbans.eu/project/#service-tools).
- Before applying the PMF on a dataset, the possible outliers have to be checked by applying the lognormal law. If a value is detected as a possible outlier, this does not mean that the value is invalid (QA/QC measures should apply), but uncommon concentrations considered as outliers disrupt the performance of the PMF analysis and have to be ignored from the database used for PMF.
- QA/QC measures based on ACTRIS guideline (ACTRIS, 2018) should apply before running PMF to be sure about the good quality of the measurement data. The quality of data can be checked using the ACTRIS QA Tool called @VOC@ developed by EMPA in the framework of ACTRIS-CiGas.

The principle consists in plotting species mixing ratio time series, xy scatterplots, seasonal and yearly comparisons, etc. This procedure is described in the ACTRIS guideline for key VOCs (ACTRIS, 2018). Afterwards, during PMF analysis, each compound will be considered "strong", "weak", or "bad" depending on its measurement quality and S/N ratio (Signal/Noise).

- If a specific compound has very high concentration values, much higher than the other VOCs, it should be treated differently (subtraction of the background or other statistical analysis) and should not be considered in the VOC database used for PMF, but as ancillary data.
- We recommend that the uncertainties calculated for the PMF analysis should follow the ACTRIS guideline (ACTRIS, 2018) since they have an impact on the weight attributed by the PMF to a measurement. Then, a harmonization of the uncertainty's calculation method is useful to compare the source apportionment studies from different measurement sites.
- When determining the optimal number of factors, several parameters (like maximum individual column mean (IM) and standard deviation (IS) of standardized residuals) were plotted versus the number of factors to determine the best solution following the method from Lee et al. (1999) and Hopke (2000). The r^2 between model and measurement should also be checked. For each *n+1* factor, it is important to verify how the fingerprint of the previous factors has changed to generate a new factor, and how independent the factors are between them. The determination of the optimal solution is finding the right balance between these parameters.
- When the optimal number of factors has been decided it is important to check the r^2 between all factors. If there is a correlation between some factors the determination of an optimal F_{Peak} (Hopke, 2000) value can help on establishing independency and stability of the factors.
- Bootstrapping PMF solutions is also highly advised since it provides statistical rotational ambiguity error assessment.
- For annual or multi-annual data series, the PMF is usually applied on a seasonal basis. If a season has a high proportion of missing data (higher than 50%), it is recommended to ignore the PMF analysis of this season because this could lead to a misinterpretation of the results and bad representativeness of the season.
- Where possible, it is very useful when conducting a source apportionment study to have a large variety of VOCs covering primary anthropogenic and biogenic non-methane hydrocarbons (NMHCs) but also secondary compounds (OVOCs) which contain markers helping to identify and confirm new sources.

- The use of constraints to guide the model towards the a priori knowledge of sources at the site is recommended where possible.
- The use of meteorological data (temperature, solar radiation, wind speed, and wind direction) can give the possibility to create a conditional probability function (CPF) plots based on wind speed and direction, which could help in identifying the sources of various factors, such as specific industries, given their specific location. Dispersion-normalized PMF (DN-PMF) can be applied to decrease the impact of atmospheric dispersion, by using the mixed layer height and mean wind speed. Temperature and solar radiation correlation help in the identification of secondary and biogenic sources.
- Correlations with other pollutants, such as NO_x (NO_2 + NO), O_3, CO, and SO_2, organic aerosols, and heavy metals, could further aid in the identification of various sources. For instance, NO_x and CO are clear indicators of anthropogenic activities.
- It must be mentioned that most of the VOC source apportionment studies are conducted on the observed VOC concentrations instead of the initial VOC concentrations. Many VOCs, especially alkenes and aromatics, have a substantial decrease from photochemical loss, and therefore their contribution might be underestimated. Although, this did not hinder the source identification, it is important to assess the impact of photochemistry on the dataset before.

6. REFERENCES

ACTRIS, C. for A.I.-S.M., Preliminary, 2021. Preliminary ACTRIS recommendation for aerosol in-situ sampling, measurements, and analysis. https://www.actris.eu/sites/default/files/2021-06/Preliminary%20ACTRIS%20recommendations%20for%20aerosol%20in-situ%20measurements%20June%202021.pdf

Akhtar, U.S., McWhinney, R.D., Rastogi, N., Abbatt, J.P., Evans, G.J., Scott, J.A., 2010. Cytotoxic and proinflammatory effects of ambient and source-related particulate matter (PM) in relation to the production of reactive oxygen species (ROS) and cytokine adsorption by particles, Inhal. Toxicol., 22, 37–47; https://doi.org/10.3109/08958378.2010.518377, 2010.

Amato, F., Hopke, P.K., 2012. Source apportionment of the ambient PM2.5 across St. Louis using constrained positive matrix factorization, Atmos. Environ., 46, 329-337; https://doi.org/10.1016/j.atmosenv.2011.09.062.

Amato, F., Alastuey, A., Karanasiou, A., Lucarelli, F., Nava, S., Calzolai, G., Severi, M., … &, Querol, X., 2016. AIRUSE-LIFE+: a harmonized PM speciation and source apportionment in five southern European cities, Atmos. Chem. Phys., 16, 3289–3309; https://doi.org/10.5194/acp-16-3289-2016.

Ayres, J.G., Borm, P., Cassee, F. R., Castranova, V., Donaldson, K., Ghio, A., Harrison, R. M., … & Froines, J., 2008. Evaluating the toxicity of airborne particulate matter and nanoparticles by measuring oxidative stress potential – A workshop report and consensus statement, Inhal. Toxicol., 20, 75–99; https://doi.org/10.1080/08958370701665517.

Badol, C., Locoge, N., Léonardis, T., & Galloo, J. C., 2008. Using a source-receptor approach to characterise VOC behaviour in a French urban area influenced by industrial emissions Part I: Study area description, data set acquisition and qualitative data analysis of the data set, Sci. Total Environ., 389, 2–3, 441–452; https://doi.org/10.1016/j.scitotenv.2007.09.003.

Balduzzi, S., Rücker, G., Schwarzer, G., 2019. How to perform a meta-analysis with R: a practical tutorial, Evid.-Bas. Ment. Health, 22, 153–160; https://doi.org/10.1136/ebmental-2019-300117.

Basnet, S., Hartikainen, A., Virkkula, A., Yli-Pirilä, P., Kortelainen, M., Suhonen, H., Kilpeläinen, L., Ihalainen, M., Väätäinen, S., Louhisalmi, J., Somero, M., Tissari, J., Jakobi, G., Zimmermann, R., Kilpeläinen, A., and Sippula, O.: Contribution of brown carbon to light absorption in emissions of European residential biomass combustion appliances, Atmos. Chem. Phys., 24, 3197–3215, https://doi.org/10.5194/acp-24-3197-2024, 2024.

Bates, J. T., Weber, R. J., Abrams, J., Verma, V., Fang, T., Klein, M., Strickland, M. J., Sarnat, S. E., Chang, H. H., Mulholland, J. A., Tolbert, P. E., and Russell, A. G., 2015. Reactive Oxygen Species Generation Linked to Sources of Atmospheric Particulate Matter and Cardiorespiratory Effects, Environ. Sci. Technol., 49, 13605–13612; https://doi.org/10.1021/acs.est.5b02967.

Baudic, A., Gros, V., Sauvage, S., Locoge, N., Sanchez, O., Sarda-Estève, R., Kalogridis, C., Petit, J. E., Bonnaire, N., Baisnée, D., Favez, O., Albinet, A., Sciare, J., Bonsang, B., 2016. Seasonal variability and source apportionment of volatile organic compounds (VOCs) in the Paris megacity (France), Atmos. Chem. Phys., 16, 18, 11961–11989; https://doi.org/10.5194/acp-16-11961-2016.

Beddows, D.C., Dall'Osto, M., Harrison, R.M., 2009. Cluster analysis of rural, urban, and curbside atmospheric particle size data, Environ. Sci. Technol., 43 (13), 4694-700; http://dx.doi.org/10./es803121t.

Beddows, D.C.S., Harrison, R.M., Green, D.C., Fuller, G.W, 2015. Receptor modelling of both particle composition and size distribution from a background site in London, UK, Atmos. Chem. Phys., 15, 10107–10125; https://doi.org/10.5194/acp-15-10107-2015.

Belis, C.A., Karagulian, F., Larsen, B.R., Hopke, P.K., 2013. Critical review and meta-analysis of ambient particulate matter source apportionment using receptor models in Europe, Atmos. Environ., 69, 94–108; https://doi.org/10.1016/j.atmosenv.2012.11.009. 1021.

Belis, C.A., Favez, O., Mircea, M., Diapouli, E., Manousakas, M.I., Vratolis, S., Gilardoni, S., Paglione, M., Decesari, S., Mocnik, G., Mooibroek, D., Salvador, P., Takahama, S., Vecchi, R., Paatero, P.,

2019. European guide on air pollution source apportionment with receptor models - Revised version 2019. EUR 29816 EN. Joint Research Centre (European Commission). JRC117306. Publications Office of the European Union, Luxembourg, 2019; https://data.europa.eu/doi/10.2760/439106.

Bhattu, D., Tripathi, S. N., Bhowmik, H. S., Moschos, V., Lee, C. P., Rauber, ...& Prévôt, A.S.H., 2024. Local incomplete combustion emissions define the PM2.5 oxidative potential in Northern India, Nature Comm., 15, 3517; http://dx.doi.org/10.1038/s41467-024-47785-5.

Bibi, Z., Coe, H., Brooks, J., Williams, P.I., Reyes-Villegas, E., Priestley, M., Percival, C.J., Allan, J.D., 2021. Technical note: A new approach to discriminate different black carbon sources by utilising fullerene and metals in positive matrix factorisation analysis of high-resolution soot particle aerosol mass spectrometer data, Atmos. Chem. Phys., 21, 10763–10777; https://doi.org/10.5194/acp-21-10763-2021.

Blanco-Donado, E.P., Schneider, I.L., Artaxo, P., Lozano-Osorio, J., Portz, L., Oliveira, M.L.S., 2022. Source identification and global implications of black carbon, Geosci. Front., 13, 101149; https://doi.org/10.1016/j.gsf.2021.101149.

Briggs, N.L., Long, C.M., 2016. Critical review of black carbon and elemental carbon source apportionment in Europe and the United States, Atmos. Environ., 144, 409–427; https://doi.org/10.1016/j.atmosenv.2016.09.002.

Borbon, A., Locoge, N., Veillerot, M., Galloo, J. C., & Guillermo, R., 2002. Characterisation of NMHCs in a French urban atmosphere: overview of the main sources, In Sci. Total Environ., 292; https://doi.org/10.1016/S0048-9697(01)01106-8.

Borlaza, L.J.S., Weber, S., Jaffrezo, J.-L., Houdier, S., Slama, R., Rieux, C., Albinet, A., Micallef, S., Trébluchon, C., Uzu, G., 2021 Disparities in particulate matter (PM10) origins and oxidative potential at a city scale (Grenoble, France) – Part 2: Sources of PM10 oxidative potential using multiple linear regression analysis and the predictive applicability of multilayer perceptron neural network analysis, Atmos. Chem. Phys., 21, 9719–9739; https://doi.org/10.5194/acp-21-9719-2021.

Brines, M., Dall'Osto, M., Beddows, D. C. S., Harrison, R. M., Querol, X., 2014. Simplifying aerosol size distribution modes simultaneously detected at four monitoring sites during SAPUSS, Atmos. Chem. Phys., 14, 2973–2986; https://doi.org/10.5194/acp-14-2973-2014.

Brines, M., Dall'Osto, M., Beddows, D.C.S., Harrison, R.M., Gómez-Moreno, F., Núñez, L., Artíñano, B., Costabile, F., Gobbi, G.P., Salimi, F., Morawska, L., Sioutas, C., Querol, X., 2015. Traffic and nucleation events as main sources of ultrafine particles in high-insolation developed world cities, Atmos. Chem. Phys., 15, 5929–5945; https://doi.org/10.5194/acp-15-5929-2015.

Calas, A., Uzu, G., Kelly, F.J., Houdier, S., Martins, J. M. F., Thomas, F., Molton, F., Charron, A., Dunster, C., Oliete, A., Jacob, V., Besombes, J.-L., Chevrier, F., Jaffrezo, J.-L., 2018. Comparison between five acellular oxidative potential measurement assays performed with detailed

chemistry on PM10 samples from the city of Chamonix (France), Atmos. Chem. Phys., 18, 7863–7875; https://doi.org/10.5194/acp-18-7863-2018.

Calas, A., Uzu, G., Besombes, J. L., Martins, J. M. F., Redaelli, M., Weber, S., Charron, A., Albinet, A., Chevrier, F., Brulfert, G., Mesbah, B., Favez, O., Jaffrezo, J. L., 2019. Seasonal variations and chemical predictors of oxidative potential (OP) of particulate matter (PM), for seven urban French sites, Atmosphere-Basel, 10, 698; https://doi.org/10.3390/atmos10110698.

Camman, J., Chazeau, B., Marchand, N., Durand, A., Gille, G., Lanzi, L., Jaffrezo, J.-L., Wortham, H., Uzu, G.,2024. Oxidative potential apportionment of atmospheric PM1: a new approach combining high-sensitive online analysers for chemical composition and offline OP measurement technique, Atmos. Chem. Phys., 24, 3257–3278; https://doi.org/10.5194/acp-24-3257-2024.

Carslaw, D.C. and Ropkins, K., 2012. Openair - an R package for air quality data analysis, Environ. Model. Software, 27 (28), 52–61; https://doi.org/10.1016/j.envsoft.2011.09.008.

CEN, 2020. CEN/TS 17434:2020, Ambient air. Determination of the particle number size distribution of atmospheric aerosol using a Mobility Particle Size Spectrometer (MPSS), European Committee for Standardization (CEN), 64 p.

CEN, 2024. EN 16976:2024, Ambient air - Determination of the particle number concentration of atmospheric aerosol. European Committee for Standardization (CEN), 54 p.

Chan, T.W., Mozurkewich, M., 2007. Simplified representation of atmospheric aerosol size distributions using absolute principal component analysis, Atmos. Chem. Phys., 7, 875–886; https://doi.org/10.5194/acp-7-875-2007.

Chen, L., Qi, X., Nie, W., Wang, J., Xu, Z., Wang, T., Liu Y., Shen, Y., Xu, Z., Kokkonen, T.V., Chi, X., Aalto, P.P., Paasonen, P., Kerminen, V.M., Petäjä, T., Kulmala, M., Ding, A., 2021. Cluster analysis of submicron particle number size distributions at the SORPES station in the Yangtze River Delta of East China, Jour. of Geop. Res.: Atmosp., 126; https://doi.org/10.1029/2020JD034004.

Chen, D.G.D., Peace, K.E., 2013. Applied meta-analysis with R (1st ed.), Chapman and Hall/CRC, 343 pp., ISBN 9780429096532; https://doi.org/10.1201/b14872.

Cheung, R. K. Y., Qi, L., Manousakas, M. I., Puthussery, J. V., Zheng, Y., Koenig, T. K., … & Modini, R. L., 2024. Major source categories of PM2.5 oxidative potential in wintertime Beijing and surroundings based on online dithiothreitol-based field measurements, Sci. Total Environ., 928, 172345; https://doi.org/10.1016/j.scitotenv.2024.172345.

Crilley, L.R., Bloss, W.J., Yin, J., Beddows, D.C.S., Harrison, R.M., Allan, J.D., Young, D.E., Flynn, M., Williams, P., Zotter, P., Prevot, A.S.H., Heal, M.R., Barlow, J.F., Halios, C.H., Lee, J.D., Szidat, S., Mohr, C., 2015. Sources and contributions of wood smoke during winter in London: Assessing local and regional influences, Atmos. Chem. Phys., 15, 3149–3171; https://doi.org/10.5194/acp-15-3149-2015.

Crobeddu, B., Aragao-Santiago, L., Bui, L. C., Boland, S., Baeza Squiban, A., 2017. Oxidative potential of particulate matter 2.5 as predictive indicator of cellular stress, Environ. Pollut., 230, 125–133; https://doi.org/10.1016/j.envpol.2017.06.051.

Cusack, M., Pérez, N., Pey, J., Alastuey, A., Querol, X., 2013. Source apportionment of fine PM and sub-micron particle number concentrations at a regional background site in the western Mediterranean: A 2.5 year study, Atmos. Chem. Phys., 13, 10, 5173-5187; https://doi.org/10.5194/acp-13-5173-2013.

Daellenbach, K. R., Uzu, G., Jiang, J., Cassagnes, L.-E., Leni, Z., Vlachou, A., Stefenelli, G., Canonaco, F., Weber, S., Segers, A., 2020. Sources of particulate-matter air pollution and its oxidative potential in Europe, Nature, 587, 414-419; https://doi.org/10.1038/s41586-020-2902-8.

Dai, Q., Ding, J., Song, C., Liu, B., Bi, X., Wu, J., Zhang, Y., Feng, Y., Hopke, P.K., 2021.Changes in source contributions to particle number concentrations after the COVID-19 outbreak: Insights from a dispersion normalized PMF, Sci. Total Environ., 759, 143548; https://doi.org/10.1016/j.scitotenv.2020.143548.

Dall'Osto, M., Thorpe, A., Beddows, D. C. S., Harrison, R. M., Barlow, J. F., Dunbar, T., Williams, P. I., and Coe, H., 2011. Remarkable dynamics of nanoparticles in the urban atmosphere, Atmos. Chem. Phys., 11, 6623–6637; https://doi.org/10.5194/acp-11-6623-2011.

Dall'Osto, M., Beddows, D.C.S., Tunved, P., Harrison, R.M., Lupi, A., Vitale, V., Becagli, S., Traversi, R., Park, K.T., Yoon, Y.J., Massling, A., Skov, H., Lange, R., Strom, J., and Krejci, R., 2019. Simultaneous measurements of aerosol size distributions at three sites in the European high Arctic, Atmos. Chem. Phys., 19, 7377–7395; https://doi.org/10.5194/acp-19-7377-2019.

Daellenbach, K.R., Uzu, G., Jiang, J., Cassagnes, L.-E., Leni, Z., Vlachou, A., Stefenelli, G., Canonaco, F., … & Prévôt, A.S.H., 2020. Sources of particulate-matter air pollution and its oxidative potential in Europe. Nature 587, 414–419. https://doi.org/10.1038/s41586-020-2902-8

Damayanti, S., Harrison, R.M., Pope, F., Beddows, D.C.S., 2023. Limited impact of diesel particle filters on road traffic emissions of ultrafine particles, Environ. Int., 174, 107888, https://doi.org/10.1016/j.envint.2023.107888.

Debevec, C., Sauvage, S., Gros, V., Sciare, J., Pikridas, M., Stavroulas, I., Salameh, T., Leonardis, T., … & Locoge, N., 2017. Origin and variability in volatile organic compounds observed at an Eastern Mediterranean background site (Cyprus), Atmos. Chem. Phys., 17(18), 11355–11388; https://doi.org/10.5194/acp-17-11355-2017.

Debevec, C., Sauvage, S., Gros, V., Gros, V., Sciare, J., Dulac, F., & Locoge, N., 2021. Seasonal variation and origins of volatile organic compounds observed during 2 years at a western Mediterranean remote background site (Ersa, Cape Corsica), Atmos. Chem. Phys., 21, 3, 1449–1484; https://doi.org/10.5194/acp-21-1449-2021.

Deng, M., Chen, D., Zhang, G., Cheng, H., 2022. Policy-driven variations in oxidation potential and source apportionment of PM2.5 in Wuhan, central China, Sci. Total Environ., 853, 158255; https://doi.org/10.1016/j.scitotenv.2022.158255.

Dinh Ngoc Thuy, V. D., Jaffrezo, J.-L., Hough, I., Dominutti, P. A., Salque Moreton, G., Gille, G., Francony, F., Patron-Anquez, A., Favez, O., Uzu, G., 2024. Unveiling the optimal regression model for source apportionment of the oxidative potential of PM10, Atmos. Chem. Phys., 24, 7261–7282; https://doi.org/10.5194/acp-24-7261-2024.

Dinoi, A., Gulli, D., Ammoscato, I., Calidonna, C.R., Contini, D., 2021. Impact of the Coronavirus Pandemic Lockdown on Atmospheric Nanoparticle Concentrations in Two Sites of Southern Italy, Atmosp., 12, 352; https://doi.org/10.3390/atmos12030352.

Dominutti, P. A., Borlaza, L., Sauvain, J. J., Ngoc Thuy, V. D., Houdier, S., Suarez, G., Jaffrezo, J. L., Tobin, S., Trébuchon, C., Socquet, S., Moussu, E., Mary, G., Uzu, G., 2023. Source apportionment of oxidative potential depends on the choice of the assay: insights into 5 protocols comparison and implications for mitigation measures, Environ. Sci. Atmos., 3, 1497–1512; https://doi.org/10.1039/d3ea00007a.

Dufresne, M., 2022. Sources et déterminants des composés organiques volatils à Marseille [École des Mines de Douai]; https://theses.hal.science/tel-04018229.

Elangasinghe, M. A., Singhal, N., Dirks, K. N., Salmond, J. A., 2014. Development of an ANN–based air pollution forecasting system with explicit knowledge through sensitivity analysis, Atmos. Pollut. Res., 5, 696–708; https://doi.org/10.5094/APR.2014.079.

Eleftheriadis, K., Gini, M.I., Diapouli, E., Vratolis, S., Vasilatou, V., Fetfatzis, P., Manousakas, M.I., 2021. Aerosol microphysics and chemistry reveal the COVID19 lockdown impact on urban air quality, Sci. Rep., 11, 14477; https://doi.org/10.1038/s41598-021-93650-6.

Fadel, M., Courcot, D., Delmaire, G., Roussel, G., Afif, C., Ledoux, F., 2023. Source apportionment of PM2.5 oxidative potential in an East Mediterranean site, Sci. Total Environ., 900, 165843; https://doi.org/10.1016/j.scitotenv.2023.165843.

Favez, O., Cachier, H., Sciare, J., Sarda-Estève, R., Martinon, L., 2009. Evidence for a significant contribution of wood burning aerosols to PM2.5 during the winter season in Paris, France; Atmos. Environ., 43, 3640–3644; https://doi.org/10.1016/j.atmosenv.2009.04.035.

Ferrero, L., Bernardoni, V., Santagostini, L., Cogliati, S., Soldan, F., Valentini, S., Massabò, D., Močnik, G., Gregorič, A., Rigler, M., Prati, P., Bigogno, A., Losi, N., Valli, G., Vecchi, R., Bolzacchini, E., 2021. Consistent determination of the heating rate of light-absorbing aerosol using wavelength- and time-dependent Aethalometer multiple-scattering correction, Sci. Total Environ., 791; https://doi.org/10.1016/j.scitotenv.2021.148277.

Fourtziou, L., Liakakou, E., Stavroulas, I., Theodosi, C., Zarmpas, P., Psiloglou, B., Sciare, J., Maggos, T., Bairachtari, K., Bougiatioti, A., Gerasopoulos, E., Sarda-Estève, R., Bonnaire, N., Mihalopoulos, N., 2017. Multi-tracer approach to characterize domestic wood burning in Athens (Greece) during wintertime, Atmos. Environ., 148, 89–101; https://doi.org/10.1016/j.atmosenv.2016.10.011.

Gaimoz, Ć., Sauvage, S., Gros, V., Herrmann, F., Williams, J., Locoge, N., Perrussel, O., Bonsang, B., D'Argouges, O., Sarda-Estve, R., & Sciare, J., 2011. Volatile organic compounds sources in Paris in spring 2007. Part II: Source apportionment using positive matrix factorisation, Environ. Chem., 8,

1, 91–103. https://doi.org/10.1071/EN10067.

Garcia-Marlès, M., Lara, R., Reche, C., Pérez, N., Tobías, A., Savadkoohi, M., Beddows, D., … & Querol, X., 2024a. Inter-annual trends of ultrafine particles in urban Europe, Environ. Int., 185, 108510; https://doi.org/10.1016/j.envint.2024.108510.

Garcia-Marlès, M., Lara, R., Reche, C., Pérez, N, Tobías, A., Savadkoohi, M., Beddows, D., … & Querol, X., 2024b. Source apportionment of ultrafine particles in urban Europe, Environ. Int., (Submitted)

Garg, S., Chandra, B.P., Sinha, V., Sarda-Esteve, R., Gros, V., Sinha, B., 2016. Limitation of the Use of the Absorption Angstrom Exponent for Source Apportionment of Equivalent Black Carbon: A Case Study from the North West Indo-Gangetic Plain, Environ. Sci. Technol., 50, 814–824; https://doi.org/10.1021/acs.est.5b03868.

Glojek, K., Dinh Ngoc Thuy, V., Weber, S., Uzu, G., Manousakas, M., Elazzouzi, R., Džepina, K., Darfeuil, S., Ginot, P., Jaffrezo, J.L., Žabkar, R., Turšič, J., Podkoritnik, A., Močnik, G., 2024. Annual variation of source contributions to PM10 and oxidative potential in a mountainous area with traffic, biomass burning, cement-plant and biogenic influences. Environ. Int. 189, 108787. https://doi.org/10.1016/j.envint.2024.108787

Godri, K. J., Harrison, R. M., Evans, T., Baker, T., Dunster, C., Mudway, I. S., Kelly, F. J., 2011. Increased oxidative burden associated with traffic component of ambient particulate matter at roadside and Urban background school sites in London, PLoS One, 6, e21961; https://doi.org/10.1371/journal.pone.0021961.

Grange, S.K., Uzu, G., Weber, S., Jaffrezo, J., Hueglin, C., 2022. Linking Switzerland's PM;10 and PM2.5 oxidative potential (OP) with emission sources. Atmospheric Chem. Phys. 22, 7029–7050. https://doi.org/10.5194/acp-22-7029-2022

Grange, S K.., Lötscher, H., Fischer, A., Emmenegger, L., Hueglin, C., 2020. Evaluation of equivalent black carbon source apportionment using observations from Switzerland between 2008 and 2018, Atmos. Meas. Tech., 13, 1867–1885; https://doi.org/10.5194/amt-13-1867-2020.

Gregorič, A., Drinovec, L., JeÅ3/4ek, I., Vaupotič, J., Grauf, D., Wang, L., Stanič, S., 2020. The determination of highly time-resolved and source-separated black carbon emission rates using radon as a tracer of atmospheric dynamics, Atmos. Chem. Phys., 20, 14139–14162; https://doi.org/10.5194/acp-20-14139-2020.

Gu, J., Pitz, M., Schnelle-Kreis, J., Diemer, J., Reller, A., Zimmermann, R., Soentgen, J., Stoelzel, M., Wichmann, H.E., Peters, A., Cyrys, J., 2011. Source apportionment of ambient particles: Comparison of positive matrix factorization analysis applied to particle size distribution and chemical composition data, Atmos. Environ., 45, 10, 1849-1857; https://doi.org/10.1016/j.atmosenv.2011.01.009.

Hamilton, S.D., Harley, R.A., 2021. High-Resolution Modeling and Apportionment of Diesel-Related Contributions to Black Carbon Concentrations, Environ. Sci. Technol., 55, 12250–12260; https://doi.org/10.1021/acs.est.1c03913.

Harrison, R.M., Beddows, D.C.S., Dall'Osto, M., 2011. PMF analysis of wide-range particle size spectra collected on a major highway, Environ. Sci. Technol., 45, 5522–5528; https://doi.org/10.1021/es2006622.

Harrison, R.M., Beddows, D.C.S., Jones, A.M., Calvo, A., Alves, C., Pio, C., 2013. An evaluation of some issues regarding the use of aethalometers to measure woodsmoke concentrations, Atmos. Environ., 80, 540–548; https://doi.org/10.1016/j.atmosenv.2013.08.026.

Helin, A., Niemi, J. V., Virkkula, A., Pirjola, L., Teinilä, K., Backman, J., Aurela, M., Saarikoski, S., Rönkkö, T., Asmi, E., Timonen, H., 2018. Characteristics and source apportionment of black carbon in the Helsinki metropolitan area, Finland, Atmos. Environ., 190, 87–98; https://doi.org/10.1016/j.atmosenv.2018.07.022.

Helin, A., Virkkula, A., Backman, J., Pirjola, L., Sippula, O., Aakko-Saksa, P., Väätäinen, S., … & Timonen, H., 2021. Variation of Absorption Ångström Exponent in Aerosols From Different Emission Sources, J. Geophys. Res. Atmos., 126, 1–21; https://doi.org/10.1029/2020JD034094.

Hellén H., Hakola H. and Laurila T., 2003. Source contributions of NMHCs in Helsinki using chemical mass balance (CMB) and multivariate (Unmix) receptor models. Atmospheric Environment, 37, 1413-1424.

Hellén H., Hakola H., Pirjola L., Laurila T. and Pystynen K.-H., 2006. Ambient air concentrations, source profiles and source apportionment of 71 different C2-C10 volatile organic compounds in urban and residential areas of Finland. Environmental Science and Technology, 40, 103-108.

Hellén H., Tykkä T. and Hakola H., 2012. Importance of isoprene and monoterpenes in urban air in Northern Europe. Atmospheric Environment, 59, 59-66.

Hellén, H., Kouznetsov, R., Kraft, K., Seppälä, J., Vestenius, M., Jalkanen, J.-P., Laakso, L., and Hakola, H., 2024. Shipping and algae emissions have a major impact on ambient air mixing ratios of non-methane hydrocarbons (NMHCs) and methanethiol on Utö Island in the Baltic Sea, Atmos. Chem. Phys., 24, 4717–4731, https://doi.org/10.5194/acp-24-4717-2024.

Hopke, P. K., 2000. A Guide to Positive Matrix Factorization, 16 pp., U-EPA, https://www3.epa.gov/ttnamti1/files/ambient/pm25/workshop/laymen.pdf.

Hopke, P.K., 2016. Review of receptor modeling methods for source apportionment, J. Air Waste Manag. Assoc., 66, 237–259; https://doi.org/10.1080/10962247.2016.1140693.

Hopke, P.K., Feng, Y., Dai, Q., 2022. Source apportionment of particle number concentrations: A global review, Sci. Total Environ., 819, 153104; https://doi.org/10.1016/j.scitotenv.2022.153104.

Hopke, P.K., Chen, Y., Rich, D.Q., Mooibroek, D., Sofowote, U.M., 2023. The application of positive matrix factorization with diagnostics to BIG DATA, Chemom. Intell. Lab. Syst., 240, 104885; https://doi.org/10.1016/j.chemolab.2023.104885.

Hopke, P.K., Chen, Y., Chalupa, D.C., Rich, D.Q., 2024. Long term trends in source apportioned particle number concentrations in Rochester NY, Environ. Pollut., 347, 123708; https://doi.org/10.1016/j.envpol.2024.123708.

in't Veld, M., Pandolfi, M., Amato, F., Pérez, N., Reche, C., Dominutti, P., Jaffrezo, J., Alastuey, A., Querol, X., Uzu, G., 2023. Discovering oxidative potential (OP) drivers of atmospheric PM10, PM2.5, and PM1 simultaneously in North-Eastern Spain, Sci. Total Environ., 857, 159386; https://doi.org/10.1016/j.scitotenv.2022.159386.

in'tVeld, M., Seco, R., Reche C., Pérez, N., Alastuey, A., Portillo-Estrada, M., Janssens, I.A., Peñuelas, J., Fernandez-Martinez, M., Marchand, N., Temime-Roussel, B., Querol, X., Yáñez-Serrano, A.M. 2024. Identification of volatile organic compounds and their sources driving ozone and secondary organic aerosol formation in NE Spain, Sci. Total Environ., 906, 167159; https://doi.org/10.1016/j.scitotenv.2023.167159.

Jafar, H.A., Harrison, R.M., 2021. Spatial and temporal trends in carbonaceous aerosols in the United Kingdom, Atmos. Pollut. Res., 12, 295–305; https://doi.org/10.1016/j.apr.2020.09.009.

Kaskaoutis, D.G., Grivas, G., Stavroulas, I., Bougiatioti, A., Liakakou, E., Dumka, U.C., 1202 Gerasopoulos, E., Mihalopoulos, N., 2021. Apportionment of black and brown carbon spectral absorption sources in the urban environment of Athens, Greece, during winter. Science of The Total Environment, 149739. https://doi.org/10.1016/j.scitotenv.2021.149739

Khan, M.F., Latif, M.T., Amil, N., Juneng, L., Mohamad, N., Nadzir, M.S., Hoque, H.M., 2015. Characterization and source apportionment of particle number concentration at a semi-urban tropical environment, Environ. Sci. Pollut. Res. Int., 22, 17, 13111-26; http://dx.doi.org/10.1007/s11356-015-4541-4.

Krecl, P., Targino, A.C., Johansson, C., 2011. Spatiotemporal distribution of light-absorbing carbon and its relationship to other atmospheric pollutants in Stockholm, Atmos. Chem. Phys., 11, 11553–11567; https://doi.org/10.5194/acp-11-11553-2011.

Kumar, S., Wang, S., Lin, N., Chantara, S., Lee, C., Thepnuan, D., 2020. Black carbon over an urban atmosphere in northern peninsular Southeast Asia : Characteristics , source apportionment , and associated health risks *, Environ. Pollut., 259, 113871; https://doi.org/10.1016/j.envpol.2019.113871.

Kutzner, R.D., von Schneidemesser, E., Kuik, F., Quedenau, J., Weatherhead, E.C., Schmale, J., 2018. Long-term monitoring of black carbon across Germany, Atmos. Environ., 185, 41–52; https://doi.org/10.1016/j.atmosenv.2018.04.039.

Laborde, M., Crippa, M., Tritscher, T., Jurányi, Z., Decarlo, P.F., Temime-Roussel, B., Marchand, N., Eckhardt, S., Stohl, A., Baltensperger, U., Prévôt, A.S.H., Weingartner, E., Gysel, M., 2013. Black carbon physical properties and mixing state in the European megacity Paris, Atmos. Chem. Phys., 13, 5831–5856; https://doi.org/10.5194/acp-13-5831-2013.

Languille, B., Gros, V., Petit, J. E., Honoré, C., Baudic, A., Perrussel, O., Foret, G., Michoud, V., Truong, F., , … & M., Favez, O., 2020. Wood burning: A major source of Volatile Organic Compounds during wintertime in the Paris region, Sci. Total Environ., 711; https://doi.org/10.1016/j.scitotenv.2019.135055.

Lanz, V. A., Hueglin, C., Buchmann, B., Hill, M., Locher, R., Staehelin, J., & Reimann, S., 2008. Receptor modeling of C2–C7 hydrocarbon sources at an urban background site in Zurich, Switzerland: changes between 1993–1994 and 2005–2006, Atmos. Chem. Phys., 8, 9, 2313–2332; https://doi.org/10.5194/acp-8-2313-2008.

Lee, E., Chan, C. K., and Paatero, P.: Application of positive matrix factorization in source apportionment of particulate pollutants in Hong Kong, Atmos. Environ., 33, 3201–3212; https://doi.org/10.1016/S1352-2310(99)00113-2, 1999.

Leni, Z., Cassagnes, L. E., Daellenbach, K. R., Haddad, I. El, Vlachou, A., Uzu, G., Prévôt, A. S. H., Jaffrezo, J. L., Baumlin, N., Salathe, M., Baltensperger, U., Dommen, J., Geiser, M., 2020. Oxidative stress-induced inflammation in susceptible airways by anthropogenic aerosol, PLoS One, 15, e0233425; https://doi.org/10.1371/journal.pone.0233425.

Leuchner, M., Gubo, S., Schunk, C., Wastl, C., Kirchner, M., Menzel, A., & Plass-Dülmer, C., 2015. Can positive matrix factorization help to understand patterns of organic trace gases at the continental Global Atmosphere Watch site Hohenpeissenberg?, Atmos. Chem. Phys., 15, 3, 1221–1236; https://doi.org/10.5194/acp-15-1221-2015.

Li, N., Xia, T., Nel, A. E., 2008. The role of oxidative stress in ambient particulate matter-induced lung diseases and its implications in the toxicity of engineered nanoparticles, Free Radic. Biol. Med., 44, 1689–1699; https://doi.org/10.1016/j.freeradbiomed.2008.01.028.

Li, J., Liu, C., Yin, Y., Kumar, K.R., 2016. Numerical investigation on the Ångström exponent of black carbon aerosol, J. Geophys. Res. Atmos., 121, 3506–3518; https://doi.org/10.1002/2015jd024718.

Liakakou, E., Stavroulas, I., Kaskaoutis, D.G., Grivas, G., Paraskevopoulou, D., Dumka, U.C., Tsagkaraki, M., Bougiatioti, A., Oikonomou, K., Sciare, J., Gerasopoulos, E., Mihalopoulos, N., 2020. Long-term variability, source apportionment and spectral properties of black carbon at an urban background site in Athens, Greece, Atmos. Environ., 222, 117137; https://doi.org/10.1016/j.atmosenv.2019.117137.

Liu, C., Chung, C.E., Yin, Y., Schnaiter, M., 2018. The absorption Ångström exponent of black carbon: From numerical aspects, Atmos. Chem. Phys., 18, 6259–6273; https://doi.org/10.5194/acp-18-6259-2018.

Liu, X., Zheng, M., Liu, Y., Jin, Y., Liu, J., Zhang, B., Yang, X., Wu, Y., Zhang, T., Xiang, Y., Liu, B., Yan, C., 2022. Intercomparison of equivalent black carbon (eBC) and elemental carbon (EC) concentrations with three-year continuous measurement in Beijing, China, Environ. Res., 209, 112791; https://doi.org/10.1016/j.envres.2022.112791.

Liu, X., Hadiatullah., H., Zhang. X., Trechera., P., Savadkoohi., M., Garcia-Marlès, M., Reche, C., Pérez, N.,

Beddows, D.C.S., Salma, I., Thén, W., Kalkavouras, P., Mihalopoulos, N., … & Querol, X., 2023. Ambient air particulate total lung deposited surface area (LDSA) levels in urban Europe, Sci. Total Environ., 898, 165466; https://doi.org/10.1016/j.scitotenv.2023.165466.

Liu, Z.R., Hu, B., Liu, Q., Sun, Y., Wang, Y.S., 2014. Source apportionment of urban fine particle number concentration during summertime in Beijing, Atmos. Environ., 96, 359-369; https://doi.org/10.1016/j.atmosenv.2014.06.055.

Lodovici, M., Bigagli, E., 2011. Oxidative stress and air pollution exposure, J. Toxicol., 2011, 487074; https://doi.org/10.1155/2011/487074.

Luo, J., Li, Z., Qiu, J., Zhang, Y., Fan, C., Li, L., Wu, H., Zhou, P., Li, K., Zhang, Q., 2023. The Simulated Source Apportionment of Light Absorbing Aerosols: Effects of Microphysical Properties of Partially-Coated Black Carbon, J. Geophys. Res. Atmos., 128; https://doi.org/10.1029/2022JD037291.

Luoma, K., Niemi, J. V., Aurela, M., Lun Fung, P., Helin, A., Hussein, T., Kangas, L., Kousa, A., Rönkkö, T., Timonen, H., Virkkula, A., Petäjä, T., 2021. Spatiotemporal variation and trends in equivalent black carbon in the Helsinki metropolitan area in Finland, Atmos. Chem. Phys., 21, 1173–1189; https://doi.org/10.5194/acp-21-1173-2021.

Lyamani, H., Olmo, F.J., Foyo, I., Alados-Arboledas, L., 2011. Black carbon aerosols over an urban area in south-eastern Spain: Changes detected after the 2008 economic crisis, Atmos. Environ., 45, 6423–6432; https://doi.org/10.1016/j.atmosenv.2011.07.063.

Masiol, M., Squizzato, S., Rich, D.Q., Hopke, P.K., 2019. Long-term trends (2005–2016) of source apportioned PM2.5 across New York State, Atmos. Environ., 201, 110–120; https://doi.org/10.1016/j.atmosenv.2018.12.038.

Massabò, D., Prati, P., 2021. An overview of optical and thermal methods for the characterization of carbonaceous aerosol, Riv. del Nuo. Cim., 44, 145–192; https://doi.org/10.1007/s40766-021-00017-8.

Mbengue, S., Serfozo, N., Schwarz, J., Holoubek, I., Ziková, N., Šmejkalová, A.H., Holoubek, I., 2020. Characterization of Equivalent Black Carbon at a regional background site in Central Europe: Variability and source apportionment, Environ. Pollut., 260; https://doi.org/10.1016/j.envpol.2019.113771.

Michoud, V., Sciare, J., Sauvage, S., Dusanter, S., Léonardis, T., Gros, V., Kalogridis, C., Zannoni, N., … & Locoge, N., 2017. Organic carbon at a remote site of the western Mediterranean Basin: Sources and chemistry during the ChArMEx SOP2 field experiment, Atmos. Chem. Phys., 17 (14), 8837–8865; https://doi.org/10.5194/acp-17-8837-2017.

Milinković, A., Gregorič, A., Grgičin, V.D., Vidič, S., Penezić, A., Kušan, A.C., Alempijević, S.B., Kasper-Giebl, A., Frka, S., 2021. Variability of black carbon aerosol concentrations and sources at a Mediterranean coastal region, Atmos. Pollut. Res., 12; https://doi.org/10.1016/j.apr.2021.101221.

Minderytė, A., Pauraite, J., Dudoitis, V., Plauškaitė, K., Kilikevičius, A., Matijošius, J., Rimkus, A., Kilikevičienė, K., Vainorius, D., Byčenkienė, S., 2022. Carbonaceous aerosol source apportionment and assessment of transport-related pollution, Atmos. Environ., 279; https://doi.org/10.1016/j.atmosenv.2022.119043.

Mousavi, A., Sowlat, M.H., Hasheminassab, S., Polidori, A., Sioutas, C., 2018. Spatio-temporal trends and source apportionment of fossil fuel and biomass burning black carbon (BC) in the Los Angeles Basin, Sci. Total Environ., 640–641, 1231–1240; https://doi.org/10.1016/j.scitotenv.2018.06.022.

Mousavi, A., Sowlat, M.H., Lovett, C., Rauber, M., Szidat, S., Bo, R., Borgini, A., Marco, C. De, Ruprecht, A.A., … &, Sioutas, C., 2019. Source apportionment of black carbon (BC) from fossil fuel and biomass burning in metropolitan Milan, Italy. Atmos. Environ., 203, 252–261; https://doi.org/10.1016/j.atmosenv.2019.02.009.

Mudway, I. S., Kelly, F. J., and Holgate, S. T., 2020. Oxidative stress in air pollution research, Free Radical Bio. Med., 151, 2–6; https://doi.org/10.1016/j.freeradbiomed.2020.04.031.

Norris, G., Duvall, R., Brown, S., Bai, S., 2014. EPA Positive Matrix Factorization (PMF) 5.0 Fundamentals and User Guide. U.S. Environmental Protection Agency, Washington, DC, EPA/600/R-14/108 (NTIS PB2015-105147); https://www.epa.gov/sites/default/files/2015-02/documents/pmf_5.0_user_guide.pdf.

Ogulei, D., Hopke, P.K., Chalupa, D.C., Utell, M.J., 2007. Modeling Source Contributions to Submicron Particle Number Concentrations Measured in Rochester, New York. Aerosol Sci. Technol., 41, 179-201; http://dx.doi.org/10.1080/02786820601116012.

Oliveira, C., Alves, c., Pio, C.A., 2009. Aerosol particle size distributions at a traffic exposed site and an urban background location in Oporto, Portugal, Quim. Nova, 32, 4, 928-933; https://doi.org/10.1590/S0100-40422009000400019.

Paatero, P., Tappert, U., 1994. Positive matrix factorization: A non-negative factor model with optimal utilization of error estimates of data values, Environmetrics, 5, 111–126; https://doi.org/10.1002/env.3170050203.

Paatero, P., 1999. The Multilinear Engine: A Table-Driven, Least Squares Program for Solving Multilinear Problems, including the n-Way Parallel Factor Analysis Model, J. of Comp. and Grap. Stat., 8(4), 854–888; https://doi.org/10.2307/1390831.

Paatero, P., Hopke, P. K., 2009. Rotational tools for factor analytic models, J. Chemometr., 23, 91–100; https://doi.org/10.1002/cem.1197.

Pancras, J.P., Landis, M.S., Norris, G.A., Vedantham, R., Dvonch, J.T., 2013. Source apportionment of ambient fine particulate matter in Dearborn, Michigan, using hourly resolved PM chemical composition data, Sci. Total Environ., 15, 448, 2-13; https://doi.org/10.1016/j.scitotenv.2012.11.083.

Pandolfi, M., Ripoll, A., Querol, X., Alastuey, A., 2014. Climatology of aerosol optical properties and black carbon mass absorption cross section at a remote high-altitude site in the western Mediterranean Basin, Atmos. Chem. Phys., 14, 6443–6460; https://doi.org/10.5194/acp-14-6443-2014.

Panopoulou, A., Liakakou, E., Sauvage, S., Gros, V., Locoge, N., Bonsang, B., Salameh, T., Gerasopoulos, E., & Mihalopoulos, N., 2021. Variability and sources of non-methane

hydrocarbons at a Mediterranean urban atmosphere: The role of biomass burning and traffic emissions, Sci. Total Environ., 800; https://doi.org/10.1016/j.scitotenv.2021.149389.

Patokoski J., Ruuskanen T.M., Hellén H., Taipale R., Grönholm T., Kajos M.K., Petäjä T., Hakola H., Kulmala M. and Rinne J., 2014. Winter to spring transition and diurnal variation of VOCs in Finland in an urban background site and a rural site. Boreal Environmental Research. 19, 79-103.Petit, J.E., Dupont, J.C., Favez, O., Gros, V., Zhang, Y., Sciare, J., Simon, L., Truong, F., Bonnaire, N., Amodeo, T., Vautard, R., Haeffelin, M., 2021. Response of atmospheric composition to COVID-19 lockdown measures during spring in the Paris region (France), Atmos. Chem. Phys., 21, 22, 17167-17183; https://doi.org/10.5194/acp-21-17167-2021.

Pey, J., Querol, X., Alastuey, A., Rodríguez, S., Putaud, J.P., Van Dingenen, R., 2009. Source Apportionment of urban fine and ultrafine particle number concentration in a Western Mediterranean city, Atmos. Environ., 43, 4407–4415; https://doi.org/10.1016/j.atmosenv.2009.05.024.

Pokorná, P., Leoni, C., Schwarz, J., Ondráček, J., Ondráčková, L., Vodička, P., Zíková, N., Moravec, P., Bendl, J., Klán, M., Hovorka, J., Zhao, Y., Cliff, S.S., Ždímal, V., Hopke, P.K., 2020. Spatial-temporal variability of aerosol sources based on chemical composition and particle number size distributions in an urban settlement influenced by metallurgical industry, Environ. Sci. Pollut. Res., 27, 38631–38643; https://doi.org/10.1007/s11356-020-09694-0.

Polissar, A.V., Hopke, P.K., Paatero, P., 1998. Atmospheric aerosol over Alaska - 2. Elemental composition and sources, J. Geophys. Res. Atmos., 103, 19045-19057; https://doi.org/10.1029/98JD01212.

Putaud, J.P., Pozzoli, L., Pisoni, E., Martins Dos Santos, S., Lagler, F., Lanzani, G., Dal Santo, U., Colette, A., 2021. Impacts of the COVID-19 lockdown on air pollution at regional and urban background sites in northern Italy, Atmos. Chem. Phys., 21, 7597–7609; https://doi.org/10.5194/acp-21-7597-2021.

Putaud, J.P., Pisoni, E., Mangold, A., Hueglin, C., Sciare, J., Pikridas, M., Savvides, C., Ondracek, J., … &Aas, W., 2023. Impact of 2020 COVID-19 lockdowns on particulate air pollution across Europe, Atmos. Chem. Phys., 23, 10145–10161; https://doi.org/10.5194/acp-23-10145-2023.

Reimann, S., Wegener, R., Claude, A., and Sauvage, S., 2000. ACTRIS: Released Measurement Guideline for VOCs and NOx, 2 pp; https://www.actris.eu/sites/default/files/Documents/ACTRIS-2/Milestones/WP3_MS3.10.pdf.

Rivas, I., Beddows, D.C.S., Amato, F., Green, D.C., Järvi, L., Hueglin, C., Reche, C., Timonen, H., Fuller, G.W., Niemi, J. V., Pérez, N., Aurela, M., Hopke, P.K., Alastuey, A., Kulmala, M., Harrison, R.M., Querol, X., Kelly, F.J., 2019. Source apportionment of particle number size distribution in urban background and traffic stations in four European cities, Environ. Int., 135, 105345; https://doi.org/10.1016/j.envint.2019.105345.

Rodríguez, S. and Cuevas, E., 2007. The contributions of “minimum primary emissions” and “new particle formation enhancements” to the particle number concentration in urban air, Aerosol Sci., 38, 1207-1219; https://doi.org/10.1016/j.jaerosci.2007.09.001.

Rusanen, A., Björklund, A., Manousakas, M. I., Jiang, J., Kulmala, M. T., Puolamäki, K., Daellenbach, K. R., 2024. A novel probabilistic source apportionment approach: Bayesian auto-correlated matrix factorization, Atmos. Meas. Tech., 17, 1251-1277; https://doi.org/10.5194/amt-17-1251-2024.

Salma, I., Németh, Z., Weidinger, T., Maenhaut, W., Claeys, M., Molnár, M., Major, I., Ajtai, T., Utry, N., Bozóki, Z., 2017. Source apportionment of carbonaceous chemical species to fossil fuel combustion, biomass burning and biogenic emissions by a coupled radiocarbon–levoglucosan marker method, Atmos. Chem. Phys., 17, 13767–13781, https://doi.org/10.5194/acp-17-13767-2017.

Salma, I., Vörösmarty, M., Gyöngyösi, A.Z., Thén, W., Weidinger, T., 2020. What can we learn about urban air quality with regard to the first outbreak of the COVID-19 pandemic? A case study from central Europe, Atmos. Chem. Phys., 20, 15725–15742; https://doi.org/10.5194/acp-20-15725-2020.

Samake, A., Uzu, G., Martins, J.M.F., Calas, A., Vince, E., Parat S., Jaffrezo, J.L., 2017. The unexpected role of bioaerosols in the Oxidative Potential of PM, Sci. Rep. ,7, 10978; https://doi.org/10.1038/s41598-017-11178-0.

Sandradewi, Jisca, Prévôt, A.S.H., Szidat, S., Perron, N., Alfarra, M.R., Lanz, V.A., Weingartner, E., Baltensperger, U.R.S., 2008. Using aerosol light abosrption measurements for the quantitative determination of wood burning and traffic emission contribution to particulate matter, Environ. Sci. Technol., 42, 3316–3323; https://doi.org/10.1021/es702253m.

Sandradewi, J., Prévôt, A.S.H., Weingartner, E., Schmidhauser, R., Gysel, M., Baltensperger, U., 2008. A study of wood burning and traffic aerosols in an Alpine valley using a multi-wavelength Aethalometer, Atmos. Environ., 42, 101–112; https://doi.org/10.1016/j.atmosenv.2007.09.034.

Sauvage, S., Plaisance, H., Locoge, N., Wroblewski, A., Coddeville, P., & Galloo, J. C., 2009. Long term measurement and source apportionment of non-methane hydrocarbons in three French rural areas, Atmos. Environ., 43, 15, 2430–2441; https://doi.org/10.1016/j.atmosenv.2009.02.001.

Savadkoohi, M., Pandolfi, M., Reche, C., Niemi, J. V, Mooibroek, D., Titos, G., Green, D.C.,…. & Querol, X., 2023. The variability of mass concentrations and source apportionment analysis of equivalent black carbon across urban Europe, Environ. Int., 178; https://doi.org/10.1016/j.envint.2023.108081.

Savadkoohi, M., Pandolfi, M., Favez, O., Putaud, J., Eleftheriadis, K., Fiebig, M., Hopke, P.K., Laj, P., … & Querol, X., 2024. Recommendations for reporting equivalent black carbon (eBC) mass concentrations based on long-term pan-European in-situ observations, Environ. Int., 185; https://doi.org/10.1016/j.envint.2024.108553.

Schaap, M., Denier van der Gon, H.A.C., 2007. On the variability of Black Smoke and carbonaceous

aerosols in the Netherlands, Atmos. Environ., 41, 5908–5920; https://doi.org/10.1016/j.atmosenv.2007.03.042.

Segersson, D., Eneroth, K., Gidhagen, L., Johansson, C., Omstedt, G., Nylén, A.E., Forsberg, B., 2017. Health impact of PM10, PM2.5 and black carbon exposure due to different source sectors in Stockholm, Gothenburg and Umea, Sweden, Int. J. Environ. Res. Public Health, 14, 11–14; https://doi.org/10.3390/ijerph14070742.

Sen, P.K., 1968. Estimates of the regression coefficient based on Kendall's Tau, J. Am. Stat. Assoc., 63(324), 1379–1389; https://doi.org/10.1080/01621459.1968.10480934.

Simon, L., 2023. Détermination des sources de composés organiques (gazeux et particulaires) en Ile-de-France. Océan, Atmosphère. Université Paris-Saclay, PhD; https://theses.hal.science/tel-04197371/file/119055_SIMON_2023_archivage.pdf.

Singh, V., Ravindra, K., Sahu, L., Sokhi, R., 2018. Trends of atmospheric black carbon concentration over United Kingdom, Atmos. Environ., 178, 148–157; https://doi.org/10.1016/j.atmosenv.2018.01.030.

Shangguan, Y., Zhuang, X., Querol, X., Li, B., Moreno, N., Trechera, P., Sola, P. C., Uzu, G., Li, J., 2022. Characterization of deposited dust and its respirable fractions in underground coal mines: Implications for oxidative potential-driving species and source apportionment, Int. J. Coal Geol., 258, 104017; https://doi.org/10.1016/j.coal.2022.104017.

Sowlat, M.H., Hasheminassab, S., Sioutas, C., 2016. Source apportionment of ambient particle number concentrations in central Los Angeles using positive matrix factorization (PMF), Atmos. Chem. Phys., 16, 4849-4866; https://doi.org/10.5194/acp-16-4849-2016.

Squizzato, S., Masiol, M., Rich, D.Q., Hopke, P.K., 2018. A long-term source apportionment of PM2.5 in New York State during 2005–2016, Atmos. Environ., 192, 35–47; https://doi.org/10.1016/j.atmosenv.2018.08.044.

Squizzato, S., Masiol, M., Emami, F., Chalupa, D.C., Utell, M.J., Rich, D.Q., Hopke, P.K., 2019. Long-Term Changes of Source Apportioned Particle Number Concentrations in a Metropolitan Area of the North-eastern United States, Atmosp., 10, 1, 27; https://doi.org/10.3390/atmos10010027.

Taghvaee, S., Sowlat, M.H., Mousavi, A., Hassanvand, M.S., Yunesian, M., Naddafi, K., Sioutas, C., 2018. Source apportionment of ambient PM2.5 in two locations in central Tehran using the Positive Matrix Factorization (PMF) model, Sci. Total Environ., 628-629, 672-686; https://doi.org/10.1016/j.scitotenv.2018.02.096.

Theil, H., 1992. A rank-invariant method of linear and polynomial regression analysis. In: Raj, B., Koerts, J. (Eds.), Henri Theil's Contributions to Economics and Econometrics, Adv. St. in Theor. and Appl. Econom., 23. Springer, Dordrecht, ISBN978-94-010-5124-8; https://doi.org/10.1007/978-94-011-2546-8_20.

Thera, B. T. P., Dominutti, P., Öztürk, F., Salameh, T., Sauvage, S., Afif, C., Çetin, B., Gaimoz, C., Keleş, M., Evan, S., Borbon, A., 2019. Composition and variability of gaseous organic pollution in the

port megacity of Istanbul: Source attribution, emission ratios, and inventory evaluation, Atmos. Chem. Phys., 19, 23, 15131–15156; https://doi.org/10.5194/acp-19-15131-2019.

Thurston, G.D., Spengler, J.D., 1985. A Multivariate Assessment of Meteorological Influences on Inhalable Particle Source Impacts, J. of Clim. and Appl. Meteor., 24, 11, 1245–1256; http://www.jstor.org/stable/26182616.

Titos, G., del Águila, A., Cazorla, A., Lyamani, H., Casquero-Vera, J.A., Colombi, C., Cuccia, E., Gianelle, V., Močnik, G., Alastuey, A., Olmo, F.J., Alados-Arboledas, L., 2017. Spatial and temporal variability of carbonaceous aerosols: Assessing the impact of biomass burning in the urban environment, Sci. Total Environ., 578, 613–625; https://doi.org/10.1016/j.scitotenv.2016.11.007.

Tobler, A.K., Skiba, A., Canonaco, F., Močnik, G., Rai, P., Chen, G., Bartyzel, J., Zimnoch, M., Styszko, K., Nęcki, J., Furger, M., Rózański, K., Baltensperger, U., Slowik, J.G., Prevot, A.S.H., 2021. Characterization of non-refractory (NR) PM1and source apportionment of organic aerosol in Kraków, Poland, Atmos. Chem. Phys., 21, 14893–14906; https://doi.org/10.5194/acp-21-14893-2021.

Trechera, P., Garcia-Marlès, M., Liu, X.S., Reche, C., Perez, N., Savadkoohi, M., Beddows, D., … & Querol, X., 2023. Phenomenology of ultrafine particle concentrations and size distribution across urban Europe, Environ. Int., 172, 107744; http://dx.doi.org/10.1016/j.envint.2023.107744.

Vanderstraeten, P., Forton, M., Brasseur, O., Offer, Z.Y., 2011. Black Carbon Instead of Particle Mass Concentration as an Indicator for the Traffic Related Particles in the Brussels Capital Region, J. Environ. Prot., 2, 525–532; https://doi.org/10.4236/jep.2011.25060.

Vestenius M., Hopke P.K., Lehtipalo K., Petäjä T., Hakola H., Hellén H., 2021. Assessing volatile organic compound sources in a boreal forest using positive matrox factorization (PMF). Atmospheric Environment, 259, https://doi.org/10.1016/j.atmosenv.2021.118503.

Via, M., Chen, G., Canonaco, F., Daellenbach, K. R., Chazeau, B., ... & Minguillón, M.C., 2022. Rolling vs. seasonal PMF: real-world multi-site and synthetic dataset comparison, Atmos. Meas. Tech., 15, 5479-5495; https://doi.org/10.5194/amt-15-5479-2022.

Viana, M., Kuhlbusch, T.A.J., Querol, X., Alastuey, A., Harrison, R.M., Hopke, P.K., Winiwarter, W., Vallius, M., … & , Hitzenberger, R., 2008. Source apportionment of particulate matter in Europe: A review of methods and results, J. Aerosol Sci., 39, 827–849; https://doi.org/10.1016/j.jaerosci.2008.05.007.

Virkkula, A., 2021. Modeled source apportionment of black carbon particles coated with a light-scattering shell, Atmos. Meas. Tech., 14, 3707–3719; https://doi.org/10.5194/amt-14-3707-2021.

Vörösmarty, M., Hopke, P. K., Salma, I., 2024. Attribution of aerosol particle number size distributions to main sources using an 11-year urban dataset, Atmos. Chem. Phys., 24, 5695–5712; https://doi.org/10.5194/acp-24-5695-2024.

Wang, Z.B., Hu, M., Wu, Z.J., Yue, D.L., He, L.Y., Huang, X. F., Liu, X.G., and Wiedensohler, A., 2013. Long-term measurements of particle number size distributions and the relationships with air mass history and source apportionment in the summer of Beijing, Atmos. Chem. Phys., 13, 10159–10170; https://doi.org/10.5194/acp-13-10159-2013.

Wang, Q., Liu, H., Ye, J., Tian, J., Zhang, T., Zhang, Y., Liu, S., Cao, J., 2021. Estimating Absorption Ångström Exponent of Black Carbon Aerosol by Coupling Multiwavelength Absorption with Chemical Composition, Environ. Sci. Technol. Lett., 8, 121–127; https://doi.org/10.1021/acs.estlett.0c00829.

Weber, S., Uzu, G., Calas, A., Chevrier, F., Besombes, J.-L., Charron, A., Salameh, D., Ježek, I., Močnik, G., Jaffrezo, J.-L., 2018. An apportionment method for the oxidative potential of atmospheric particulate matter sources: application to a one-year study in Chamonix, France, Atmos. Chem. Phys., 18, 9617–9629; https://doi.org/10.5194/acp-18-9617-2018.

Weber, S., Uzu, G., Favez, O., Borlaza, L. J. S., Calas, A., Salameh, D., Chevrier, F., …. & Jaffrezo, J.-L., 2021. Source apportionment of atmospheric PM10 oxidative potential: synthesis of 15 year-round urban datasets in France, Atmos. Chem. Phys., 21, 11353–11378; https://doi.org/10.5194/acp-21-11353-2021.

Wegner, T., Hussein, T., Hämeri, K., Vesala, T., Kulmala, M., Weber, S., 2012. Properties of aerosol signature size distributions in the urban environment as derived by cluster analysis, Atmos. Environ., 61, 350–360; https://doi.org/10.1016/j.atmosenv.2012.07.048.

Wehner, B., Wiedensohler, A., 2003. Long term measurements of submicrometer urban aerosols: statistical analysis for correlations with meteorological conditions and trace gases, Atmos. Chem. Phys., 3, 867–879; https://doi.org/10.5194/acp-3-867-2003.

Wiedensohler, A., Wiesner, A., Weinhold, K., Birmili, W., Hermann, M., Merkel, M., Müller, T., Pfeifer, S., Schmidt, A., Tuch, T., Velarde, F., Quincey, P., Seeger, S., Nowak, A., 2018. Mobility particle size spectrometers: Calibration procedures and measurement uncertainties, Aerosol Sci. Technol., 52, 146–164; https://doi.org/10.1080/02786826.2017.1387229.

Yáñez-Serrano, A. M., Bach, A., Bartolomé-Català, D., Matthaios, V., Seco, R., Llusià, J., Filella, I., & Peñuelas, J., 2021. Dynamics of volatile organic compounds in a western Mediterranean oak forest, Atmos. Environ., 257; https://doi.org/10.1016/j.atmosenv.2021.118447.

Yurdakul, S., Civan, M., & Tuncel, G., 2013. Volatile organic compounds in suburban Ankara atmosphere, Turkey: Sources and variability, Atmos. Res., 120–121, 298–311; https://doi.org/10.1016/j.atmosres.2012.09.015.

Zhang, G., Peng, L., Lian, X., Lin, Q., Bi, X., Chen, D., Li, M., Li, L., Wang, X., Sheng, G., 2019. An improved absorption Ångström exponent (AAE)-based method for evaluating the contribution of light absorption from brown carbon with a high-time resolution, Aerosol Air Qual. Res., 19, 15–24; https://doi.org/10.4209/aaqr.2017.12.0566.

Zhang, X., Mao, M., Chen, H., Tang, S., 2020a. The Angstrom exponents of black carbon aerosols with non-absorptive coating: A numerical investigation, J. Quant. Spectrosc. Radiat. Transf., 257,

107362; https://doi.org/10.1016/j.jqsrt.2020.107362.

Zhang, X., Mao, M., Yin, Y., Tang, S., 2020b. The absorption Ångstrom exponent of black carbon with brown coatings: Effects of aerosol microphysics and parameterization, Atmos. Chem. Phys., 20, 9701–9711; https://doi.org/10.5194/acp-20-9701-2020.

Zheng, H., Kong, S., Chen, N., Fan, Z., Zhang, Y., Yao, L., Cheng, Y., Zheng, S., Yan, Y., Liu, D., Zhao, D., Liu, C., Zhao, T., Guo, J., Qi, S., 2021. A method to dynamically constrain black carbon aerosol sources with online monitored potassium, npj Clim. Atmos. Sci., 4; https://doi.org/10.1038/s41612-021-00200-y.

Zíková, N., Wang, Y., Yang, F., Li, X., Tian, M., Hopke, P.K., 2016. On the source contribution to Beijing PM2.5 concentrations, Atmos. Environ., 134, 84-95; http://dx.doi.org/10.1016/j.atmosenv.2016.03.047.

Zotter, P., Herich, H., Gysel, M., El-Haddad, I., Zhang, Y., Mocnik, G., Hüglin, C., Baltensperger, U., Szidat, S., Prévôt, A.S.H., 2017. Evaluation of the absorption Ångström exponents for traffic and wood burning in the Aethalometer-based source apportionment using radiocarbon measurements of ambient aerosol, Atmos. Chem. Phys., 17, 4229–4249; https://doi.org/10.5194/acp-17-4229-2017.